HAW HAMBURG

Master Thesis

Mohamed Oussama Hammami

Turbofan Specific Fuel Consumption, Size, and Mass from Correlated Engine Parameters

Fakultät Technik und Informatik

Department Fahrzeugtechnik und Flugzeugbau

Faculty of Engineering and Computer Science

Department of Automotive and Aeronautical Engineering

Mohamed Oussama Hammami

Turbofan Specific Fuel Consumption, Size, and Mass from Correlated Engine Parameters

Master Thesis Submitted as Part of the Master`s Examination

Course of Study: Aeronautical Engineering
In Department: Automotive and Aeronautical Engineering
Faculty of Technology and Computer Science
Hamburg University of Applied Science

Supervising Professor: Prof. Dr.-Ing. Dieter Scholz, MSME
Second Examiner: Dr.-Ing. Daniel Nerger

Submission Date: 15.09.2021

DOI:
https://doi.org/10.15488/xxxxx

URN:
https://nbn-resolving.org/urn:nbn:de:gbv:18302-aero2021-09-15.018
Associated URLs:
https://nbn-resolving.org/html/urn:nbn:de:gbv:18302-aero2021-09-15.018

Any further request may be directed to:
Prof. Dr.-Ing. Dieter Scholz, MSME
E-Mail see: http://www.ProfScholz.de

This work is part of:
Digital Library - Projects & Theses - Prof. Dr. Scholz
http://library.ProfScholz.de

Published by
Aircraft Design and Systems Group (AERO)
Department of Automotive and Aeronautical Engineering
Hamburg University of Applied Science

This report is deposited and archived:
- Deutsche Nationalbiliothek (http://www.dnb.de)
- Repositorium der Leibniz Universität Hannover (http://www.repo.uni-hannover.de)
- Internet Archive (http://archive.org), item: https://archive.org/details/TextHammami.pdf

This report has associated published data in Harvard Dataverse:
https://doi.org/10.7910/DVN/UW6FAP

Abstract

Purpose – Simple equations and more extended models are developed to determine characteristic engine parameters: Specific fuel consumption (SFC), engine mass, and engine size characterized by engine length and diameter. SFC (c) is considered a linear function of speed: $c = c\_a * V + c\_b$.

Methodology – Data from 718 engines is collected from various open sources into an Excel spreadsheet. The characteristic engine parameters are plotted as function of bypass ratio (BPR), date of entry into service (EIS), take-off thrust, and typical cruise thrust. Engine length and diameter are plotted versus engine mass. Linear and nonlinear regression functions are investigated. Moreover, Singular Value Decomposition (SVD) is used to establish relations between parameters. SVD is used with Excel and MATLAB. The accuracy of all equations and models is compared.

Findings – SFC should be calculated as a linear function of speed. This is especially important, when SFC is extrapolated to unconventional (low) cruise speeds for jet engines. The two parameters c_a and c_b are best estimated from a logarithmic or power function of bypass ratio (BPR). SFC and c_b clearly improved over the years. Engine mass, diameter, and length are proportional to take-off thrust. Characteristic engine parameters can also be obtained from SVD with comparable accuracy. However, SVD is more complicated to set up than using a simple equation.

Practical implications – Engine characteristics need to be estimated based on only a few known parameters for aircraft preliminary sizing, conceptual design, and aircraft optimization as well as for practical quick calculations in flight mechanics. This thesis provides the tools.

Social implications – Most engine characteristics like SFC are considered company secrets. The availability of open access engine data is the first step, but wisdom is retrieved only with careful analysis of the data as done here. Openly available aircraft engineering knowledge helps to democratize the discussion about the ecological footprint of aviation.

Originality/value – Simple equation for jet engine SFC, mass, and size deduced from a large engine database are offered. This approach delivered equations as a function of BPR with an error of only 6%, which is the same accuracy as more complex equations from literature.

Keywords (LCSH)

Aeronautics, Airplanes--Fuel Consumption, Airplanes--Motors--Thrust, Aircraft Drafting--Design and Construction, Mathematical models, Singular Value Decomposition, Regression Analysis, Electronic Spreadsheets [Specific Fuel Consumption, Thrust, Engine, Mass, Diameter, Volume, Length, Aircraft Design, Sizing, Minimum Mean Square Error].

Kurzreferat

Zweck – Einfache Gleichungen und erweiterte Modelle werden entwickelt, um charakteristische Triebwerksparameter zu bestimmen: Spezifischer Kraftstoffverbrauch (SFC), Triebwerksmasse und Triebswerkgröße, gekennzeichnet durch Triebwerkslänge und -durchmesser. SFC (c) wird als lineare Funktion der Geschwindigkeit betrachtet: $c = c\_a * V + c\_b$.
Methodik – Daten von 718 Flugzeugtriebwerken werden aus verschiedenen offenen Quellen in einer Excel-Tabelle gesammelt. Die charakteristischen Triebwerksparameter wurden als Funktion des Nebenstromverhältnisses (BPR), des Datums der Indienststellung (EIS), des Startschubs und des typischen Reiseflugschubs aufgetragen. Triebwerkslänge und -durchmesser wurden als Funktion der Triebwerksmasse aufgetragen. Es werden lineare und nichtlineare Regressionsgleichungen untersucht. Darüber hinaus wurde die Singular Value Decomposition (SVD) verwendet, um Beziehungen zwischen Parametern herzustellen. SVD wird mit Excel und MATLAB verwendet. Die Genauigkeit aller Gleichungen und Modelle wird verglichen.
Ergebnisse – SFC sollte als lineare Funktion der Geschwindigkeit berechnet werden. Dies ist besonders wichtig, wenn SFC auf unkonventionelle (niedrige) Reisegeschwindigkeiten für Düsentriebwerke extrapoliert wird. Die beiden Parameter c_a und c_b werden am besten aus einer logarithmischen oder Potenzfunktion des Nebenstromerhältnisses (BPR) geschätzt. SFC und c_b haben sich über die Jahre deutlich verbessert. Triebwerksmasse, -durchmesser und -länge verhalten sich proportional zum Startschub. Mit vergleichbarer Genauigkeit können auch charakteristische Triebwerksparameter aus SVD gewonnen werden. Die Einrichtung von SVD ist jedoch komplizierter als die Verwendung einer einfachen Gleichung.
Bedeutung für die Praxis – Für die Flugzeugdimensionierung, den Flugzeugentwurf und die Flugzeugoptimierung sowie für schnelle praktische Berechnungen in der Flugmechanik müssen Triebwerkseigenschaften anhand weniger bekannter Parameter abgeschätzt werden. Die Masterarbeit stellt diese Werkzeuge zur Verfügung.
Soziale Bedeutung – Die meisten Triebwerkseigenschaften wie SFC gelten als Betriebsgeheimnisse. Die freie Verfügbarkeit von Triebwerksdaten ist der erste Schritt, aber Weisheit wird nur durch eine sorgfältige Analyse der Daten wie hier gewonnen. Offen verfügbares flugzeugtechnisches Wissen hilft, die Diskussion, um den ökologischen Fußabdruck der Luftfahrt zu demokratisieren.
Originalität / Wert – Es wurden einfache Gleichungen für SFC, Masse und Größe von Strahltriebwerken, aus einer großen Triebwerksdatenbank abgeleitet. Dieser Ansatz lieferte Gleichungen als Funktion des Nebenstromverhältnisses mit einem Fehler von nur 6 %, was der gleichen Genauigkeit entspricht, wie sie komplexere Gleichungen aus der Literatur aufweisen.

Stichworte (GND)
Luftfahrt, Luftfahrzeug, Kraftstoffverbrauch, Triebwerk, Flugzeug, Schub, Flugtriebwerk, Strahltriebwerke, Mantelstromtriebwerk, Entwurf, Singulärwertzerlegung, Regressionsanalyse, Nichtlineares mathematisches Modell, Dimensionierung, Masse, Durchmesser, Länge, Volumen, Tabellenkalkulation

HAW HAMBURG

DEPARTMENT OF AUTOMOTIVE AND AERONAUTICAL ENGINEERING

Turbofan Specific Fuel Consumption, Size, and Mass from Correlated Engine Parameters

Task for a Master Thesis

Background

The specific fuel consumption (SFC) characterizes the efficiency of an aircraft's engine. For a jet engine, the thrust specific fuel consumption is defined as the fuel mass consumed per unit thrust and per unit time. SFC changes with aircraft speed (V) and altitude (h). The knowledge of SFC is fundamental for calculations in flight mechanics and aircraft design. In aircraft design also engine mass is important, because it adds to the aircraft overall mass. Engine size is important for engine integration. Simple but reliable engine black box models are needed in aircraft analysis and design. SFC (c) can be represented by a linear function $c = c_a V + c_b$ as explained in a memo (https://purl.org/aero/M2017-07-15). The table "Civil Turbojet/Turbofan Specifications" (http://www.jet-engine.net/civtfspec.html) is an open source of input parameters, from which black box engine models can be built. An Excel version is available that also includes the year of entry into service of the engines. Consider also work from Bensel and Schulz (http://library.ProfScholz.de) and Herrmann (http://fm.ProfScholz.de).

Task

Define engine models for engine SFC, size and mass based on given data. Follow these steps:

- Start with a short literature review to appreciate previous results on the topic.
- Extend the given Excel spreadsheet with further engine data as necessary and available.
- Calculate c_a and c_b from the spreadsheet for all engines with sufficient data available.
- Work with linear and non-linear regression to find equations for engine SFC, size and mass. Consider all given engine parameters in your regression one by one and in a useful combination.
- Work with linear and non-linear regression to find equations for c_a and c_b in order to describe SFC based on the equation $c = c_a V + c_b$. This may eliminate the fundamental problem inherent in the definition of SFC based on thrust (instead based on power).
- Find models describing engine SFC, size and mass based on Singular Value Decomposition (SVD) in Excel (and MATLAB).

The report has to be written in English based on German or international standards on report writing.

Table of Contents

List of Figures

List of Tables

Nomenclature

a_0	Speed of sound
a_1	Adiabatic thermal gradient for the troposphere
C_a	Specific Fuel Consumption factor
C_b	Specific Fuel Consumption factor
C_T	Thrust Specific Fuel Consumption
$C_{T_{grd}}$	Thrust Specific Fuel Consumption at sea level
D_{Fan}	Fan Diameter
F	Maximum thrust in cruise phase
F_0	Maximum thrust at a fixed point
F_{Cruise}	Cruise Thrust
F_{TO}	Take-off Thrust
G	Gas generator power function
G_0	Gas generator power function at sea level
h	Altitude
K	Temperature function of compression process
k_1, k_2	Factors related to fundamental engine design parameters
M	Mach Number
P_0	Ambient pressure at sea level
P_{amb}	Ambient pressure
T	Temperature
T_0	Temperature at sea level
$T_{Cruise_{Tr}}$	Cruise Temperature at the troposphere
$T_{Cruise_{St}}$	Cruise temperature at the stratosphere
V	Velocity
V_{engine}	Engine Volume
m	Engine Mass
m_{TO}	Take-off Mass
x	Variable coefficient
η_c	Isentropic compressor efficiency
η_d	Isentropic fan intake duct efficiency
η_f	Isentropic fan efficiency
η_i	Gas generator intake stagnation pressor ratio
η_n	Isentropic efficiency of expansion process in the nozzle
η_t	Isentropic turbine efficiency
ε_c	Inlet / Outlet pressure ratio of the compressor on the ground
λ	Bypass Ratio
ρ	Density of the air
ρ_0	Density of the air at sea level

List of Abbreviations

BPR	Bypass-Ratio
EASA	European Union Aviation Safety Agency
FAA	Federal Aviation Administration
ISA	International Standard Atmosphere
OPR	Overall Pressure Ratio
SFC	Specific Fuel Consumption
SVD	Singular Value Decomposition
SI	International System of Units
TCA	Third Country Authority
TIT	Turbine Inlet Temperature
TSFC	Thrust Specific Fuel Consumption
PSFC	Power Specific Fuel Consumption

1 Introduction

1.1 Motivation

As is the goal of any business, airline companies aim to reduce costs wherever possible. They rely on the turbofan engine to deliver high efficiency and high thrust without consuming much fuel to carry people worldwide. The aeronautical field is always evolving, and new performant and economic turbojet engines are developed. The first step in aircraft design is to gather several parameters such as specific fuel consumption, thrust, and mass. That information is, most of the time, private and kept secret by aircraft and engine manufacturers. However, there are free internet sources providing databases with data from old engines. Engineers and researchers use these old data to create numerical models to predict modern turbojet engine design parameters. Still, these models are not 100% correct and give mixed results using different input parameters.

This analysis's primary goal is to study the linearity of specific fuel consumption, correlate between engine parameters, and create a simplified linear model with a low margin of error without forgetting that designing an aircraft balances mass, thrust, and cost.

1.2 Definitions

Specific Fuel Consumption (SFC)
Specific fuel consumption is used to characterize the engine's fuel efficiency. The "fuel consumption" means how much fuel the engine burns each hour and the "specific" is a scientific term meaning divided by pound (Newton) of thrust. Gathering the terms together, SFC means a mass of fuel burned by an engine in one hour divided by its thrust. (Mattingly 1996)

Engine Thrust
Thrust is the force that allows the aircraft to move forward. It is mainly generated from the engines of the aircraft. It is used to overcome the airplane's drag created by its body structure and mass. A reaction of accelerating a mass of gas generates a mechanical force as explained by Newton's third law. The gas is compressed and combusted inside the core of an engine and finally ejected throw the nozzle, which allows the engine to move in the opposite direction of the gas flow. (Jenkinson 1999)

Bypass Ratio (BPR)

In a turbofan engine, the gas is sucked by the fan and split into two parts. The first part of the gas is drawn into the engine core, and the second part bypass it. The bypass ratio is the ratio between the bypass stream's mass flow rate to the mass flow rate entering the core. Engine with high BPR produces a more significant amount of thrust while consuming the same fuel as a lower BPR engine. To increase the BPR, the fan diameter can be increased. However, many factors are taken into consideration during the sizing of a turbojet engine: Airflow distortion, mass, physical envelope, thrust output, fuel consumption, and cost are some of the primary design parameters that impact the choice and manufacturing of engines. (Dankanich 2017)

1.3 Objectives

This work aims to develop precise and simplified models to determine the Specific Fuel Consumption of a turbojet engine based on an open-source database containing engine models with their design parameters during Take-off and Cruise phases. The investigation will be carried out in 5 steps

- Study the linearity of SFC and calculation of its factors C_a and C_b.
- Correlate between engine parameters to understand the dependency of these parameters on each other.
- Create simplified models on Excel based on the conclusions from the previous step.
- Apply the Singular Value Decomposition method to find models for SFC.
- Compare models for both methods to evaluate which one is more accurate.

1.4 Structure

The main part of this study is structured as follows:

Chapter 2 presents the literature review's key focus, which is on previous models for calculating the specific fuel consumption and thrust.

Chapter 3 contains the analysis of engine parameters behavior. It includes the estimation of C_a and C_b, the analysis of the dependency between design parameters and the creation of SFC and thrust models using Excel tool.

Chapter 4 describes the Singular Value Decomposition method and its application to create SFC models using Excel and MATLAB.

Chapter 5 includes the conclusions and the outlook of the possibilities to improve and continue this work.

The data collected for this thesis as well as all calculations are archived in the data repository at Harvard University under https://dataverse.harvard.edu/dataverse/LibraryProfScholz. The link to the dataset of this thesis is given on page 3.

2 Literature Review

2.1 Parameters Influencing SFC and Thrust

The turbojet engine parameters depend on each other. That can be explained by the fact that a decision of one variable or parameter can affect several other parameters. The aircraft information includes the performance parameters like specific thrust, propulsive efficiency, specific fuel consumption, etc., and operating parameters which are pressure ratio, altitude, temperature, Bypass ratio, flight Mach number, and mass. The performance parameters are affected by the operating parameters. Likewise, they can also be influenced by other performance parameters. (Patel 2018)

2.1.1 SFC and Thrust Dependency on Performance Parameters

Previous research has shown that thrust and SFC vary with other flight parameters.
Mattingly (1996) mentioned that thrust and fuel consumption decreases with altitude until 11km, which is the atmosphere's isothermal layer. The author also mentioned that both primal performance parameters increase with Mach number. Moreover, if the altitude and Mach number are constant, the specific fuel consumption varies with thrust.

Different technologies and research have also been proposed and studied to optimize the turbojet engine's overall performance. Guha (2001) proposed a methodology to optimize fan pressure ratio, BPR, OPR, and TIT. A multi-point on-design method was later developed by Schutte (2009) for optimizing the aero-thermodynamic cycle of an aero engine.

Fabian (2012) mentioned that, by increasing the overall pressure ratio, a fuel burned reduction is expected, which will increase the thermal efficiency of aircraft propulsion systems. The authors used the study of addition or removal of final compressor stages in off-the-shelf engines to obtain an improvement in OPR and to evaluate the possible advantages in the thrust increase and SFC reduction.

According to Young (2005), the increase in combustor outlet temperature was the most critical factor responsible for the steady increase in gas turbine efficiency. The authors developed a thermodynamic model for cooled turbine analysis to evaluate the effects of engine parameters variation. However, there are still some questions regarding applying this technique to the most relevant aircraft flight phase's performance.

Dik (2017) described SFC's improvement by increasing the engine thermal and propulsive efficiencies, which can be realized by reducing specific thrust by increasing the fan diameter and fan flow. They studied the UltraFan 3-shaft turbofan engine, a new technology planned to be operational from 2025. The study results proved that an increment in fan diameter, BPR, OPR, and TIT resulted in a 7.3% increase in propulsive efficiencies and an 11% reduction in SFC.

Patel (2018) investigated the efficiency, thrust, and fuel consumption optimization for a turbojet engine. They have developed a jet engine's thermal model and used a multi-objective heat transfer search (MOHTS) algorithm to solve it. Furthermore, the results are obtained in the form of a set of Pareto-optimal points and represented in two-dimensional objective space compared with the results obtained by solving optimization problems.

Freire (2019) concluded that, from an overall pressure ratio study, if one high-pressure compressor stage is removed, the SFC will be decreased. Nevertheless, the strategy is not recommended due to its expensiveness. On the other hand, the author evaluated another engine modification, including a high-temperature resistance material called Ceramic matrix composites (CMC) that can implement thrust gain and reduce SFC.

2.1.2 SFC and Thrust Dependency on Operating Parameters

Thrust and SFC are usually influenced by factors such as altitude, speed, mass, and BPR. The effect of the operating parameters on thrust and SFC is significant.

Najjar (2015) calculated the variation of SFC and thrust at design points and other off-design conditions. With a reduction in flight Mach number by 10%, the authors proved that a turbojet engine's specific fuel consumption decreases by 1.46%, and the specific thrust increases by 2.35%. (Figure 2.1).

As for the altitude effect, the authors have concluded that, for an altitude higher than 11500 m, neither the specific thrust nor the specific fuel consumption is affected, which is due to the speed of sound, which remains constant after this altitude which is represented in Figure 2.2.

Furthermore, they have also found that the optimum compressor pressure ratio for a maximum specific thrust is 14, as shown in Figure 2.3. Also, the pressure ratio reduction by 10% results in a 1.34% increase in SFC and a 0.0022% decrease in thrust.

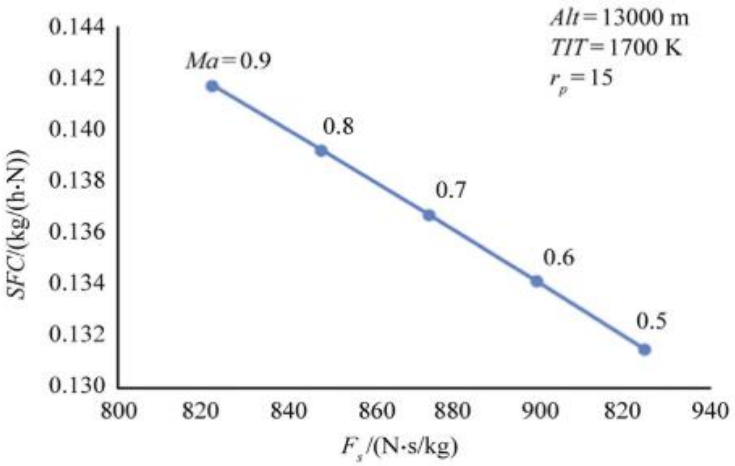

Figure 2.1 Relation of specific thrust and specific fuel consumption at design point with variable Mach Number. (Najjar 2015, page 117)

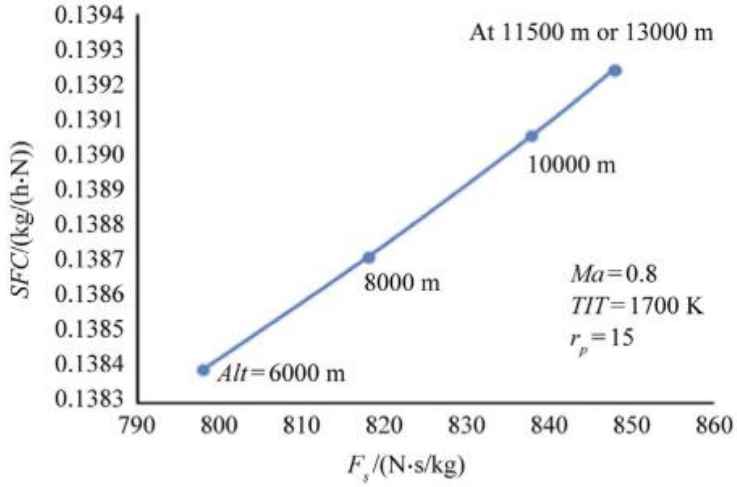

Figure 2.2 Relation of specific thrust and specific fuel consumption at design point with variable altitude. (Najjar 2015, page 117)

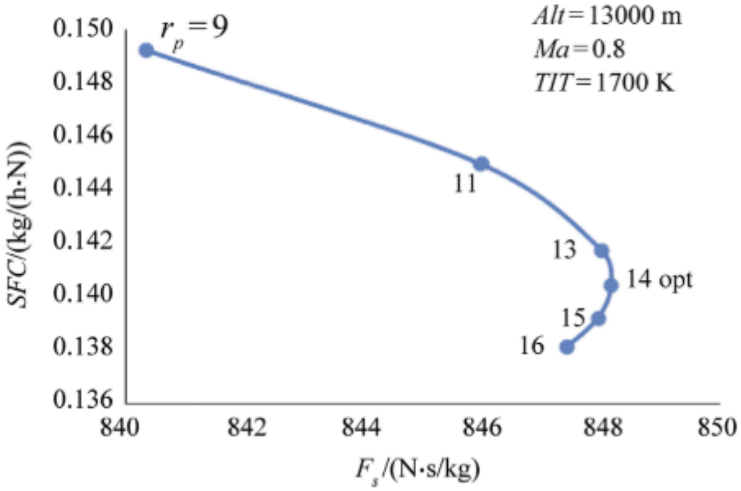

Figure 2.3 Relation of specific thrust and specific fuel consumption at design point with variable pressure ratio. (Najjar 2015, page 117)

Dankanich (2017) have studied the trend of a turbine engine when compared across an increasing BPR. From their research, the authors explained how a high BPR engine could produce a tremendous amount of thrust with low fuel consumption as a lower BPR engine. They have used a method called fixed core. This method consists of defining the free current and altitude conditions as a first step then setting up an engine with a given mass and fuel flow, but the BPR would vary from 0 to 12. The idea was to continually install an enormous fan on the front of a turbojet engine and analyze its performance. Burner and turbine properties were used in the calculation of the compressor performance. The results showed that the engine produces more thrust for the same amount of fuel as the BPR increases. Moreover, since SFC varies proportionally with the thrust, it was concluded that, as BPR increases, SFC decreases. From their calculations, the authors showed that the turbojet engine consumed roughly 1.32 pounds per pound-force per hour for a BPR equal to zero while the BPR of 12 consumed 0.7 pounds per pound-force per hour.

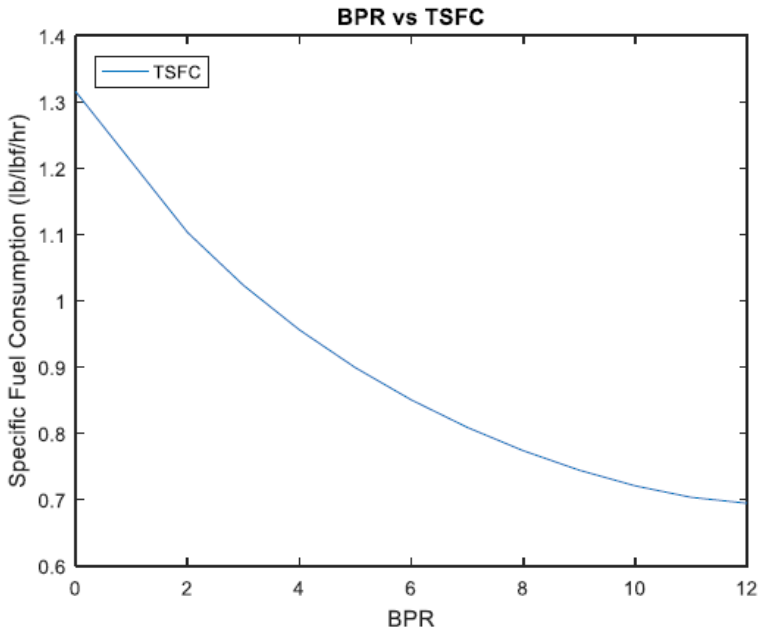

Figure 2.4 SFC as a function of BPR (Dankanich 2017, page 18)

Svoboda (2004) investigated the effect of dry weight on the take-off thrust. The author gathered engine data in a spreadsheet and sorted it by take-off thrust. The engine's BPR was at least 2.0. Afterward, many relationships between the engine parameters and take-off thrust were plotted and examined.

The author concluded that the relationship between dry weight and take-off thrust is linear and proportional.

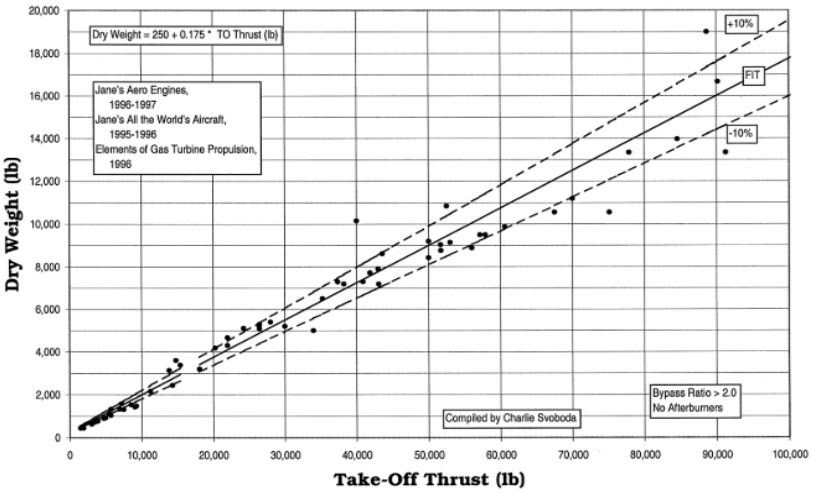

Figure 2.5 Dry weight as a function of Take-off thrust (Svoboda 2000, page 19)

Gao (2011) used MATLAB Simulink to solve the thermodynamic parameters of a micro-turbojet engine. The authors discovered that ambient temperature has a significant effect on engine parameters. With the increase of the ambient temperature, the SFC rises, and the thrust decreases.

2.2 Previous Models Calculating SFC and Thrust

2.2.1 Models for SFC Calculations

Many scientists and engineers focused on optimizing fuel consumption and the efficiency of turbojet engines. For that, many models have been created using several methods and software.

Mattingly (1996) proposed a linear model to calculate the SFC. The author concluded that the specific fuel consumption depends linearly on the Mach number. (2.1) describes this linearity.

$$SFC = (1.13 \cdot 10^{-5} + 1.25 \cdot 10^{-5} M)\sqrt{\theta} \tag{2.1}$$

where

$$\theta = \frac{T(h)}{T_0}$$

h	Altitude (m)
M	Flight Mach Number
T	Temperature for a given Altitude (K)
T_0	Temperature at sea level (K)

Based on Mattingly's model, for engines fitted to commercial aircraft, which means with a high dilution rate, this specific consumption is, in fact, not constant. In reality, SFC depends on operational flight parameters such as Mach number and altitude.

This model was later adjusted by Roux (2005) and Scholz (2017) by multiplying the constants by a factor of 0.92 (switching to SI-units) to obtain

$$SFC = C_T = C_a \cdot V + C_b \quad , \tag{2.2}$$

where

$$C_a = 3.38 \cdot 10^{-8} \frac{\text{kg}}{\text{Nm}}$$
$$C_b = 1.04 \cdot 10^{-5} \sqrt{\frac{T(h)}{T_0}} \frac{\text{kg}}{\text{Ns}} \quad .$$

Torenbeek (1997) proposed another model based on engine performance analysis.

$$SFC = 2.01 \cdot 10^{-5} \frac{\left(\phi - \mu - \frac{K}{\eta_c}\right)}{\sqrt{5\eta_n\left(1 + \eta_{tf}\lambda\right)}\sqrt{G + 0.2M^2 \frac{\eta_d}{\eta_{tf}}\lambda} - (1+\lambda)M} \tag{2.3}$$

whith

$$G = \left(\phi - \frac{K}{\eta_c}\right)\left(1 - \frac{1.01}{\eta_i^{\frac{\gamma-1}{\gamma}}(K+\mu)\left(1 - \frac{K}{\phi\eta_c\eta_t}\right)}\right)$$
$$K = \mu\left(\varepsilon_c^{\frac{\gamma-1}{\gamma}} - 1\right)$$
$$\mu = 1 + \frac{\gamma - 1}{2} M^2$$
$$\phi = \frac{T_{TE}}{T(h)}$$
$$\eta_i = 1 - \frac{0{,}7M^2(1 - \eta_{inlet})}{1 + 0{,}2M^2}$$

G	Gas generator power function
K	Temperature function of compression process (K)
T_{TE}	Turbine entry temperature in cruise
η_c	Isentropic compressor efficiency
η_d	Isentropic fan intake duct efficiency

η_f Isentropic fan efficiency

η_i Gas generator intake stagnation pressor ratio

η_n Isentropic efficiency of expansion process in the nozzle

η_t Isentropic turbine efficiency

The author confirmed with this model that SFC is an increasing and quasi-linear function of the flight Mach number (Figure 2.6). It is also stated that the Torenbeek model confirms the linearity of SFC with BPR if it is greater than 3 (Figure 2.7).

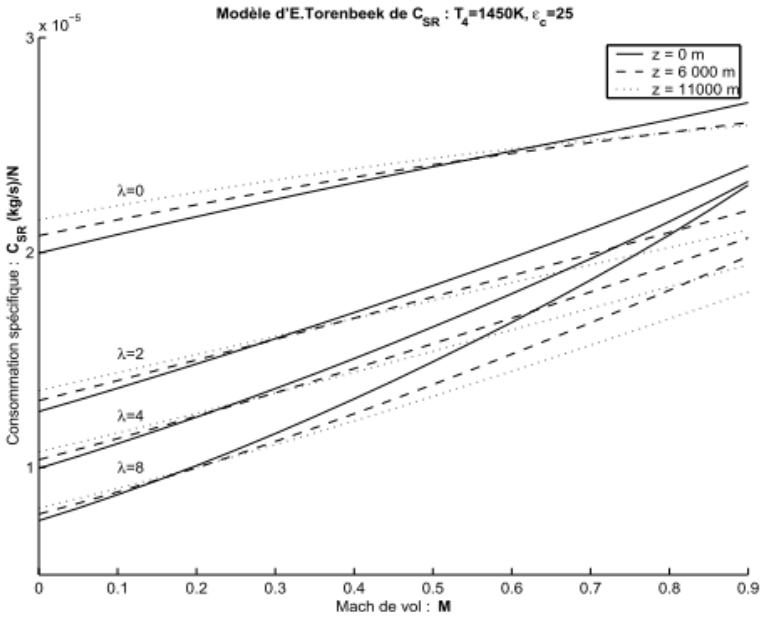

Figure 2.6 Torenbeek Model: SFC as a function of Mach number (Roux 2005, page 34)

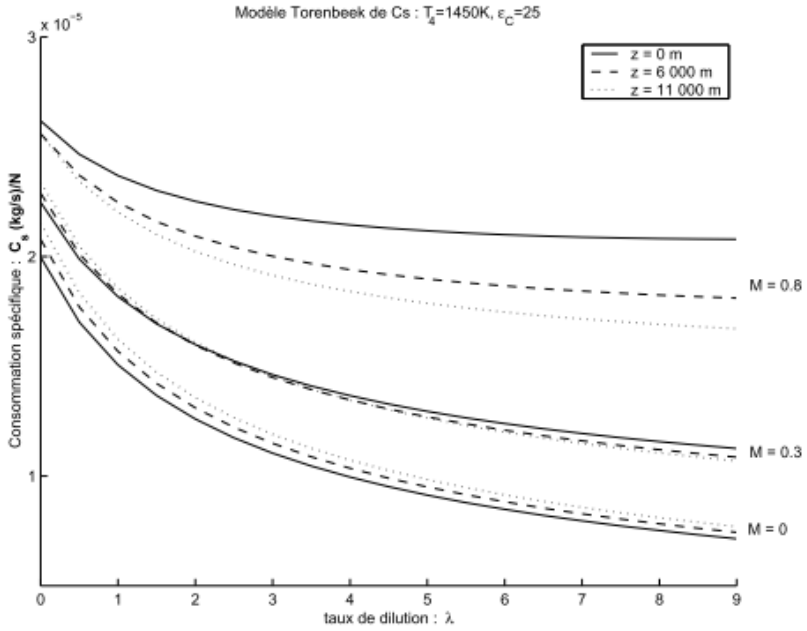

Figure 2.7 Torenbeek Model: SFC as a function of BPR (Roux 2005, page 34)

Other linear models can be used to calculate SFC. Figure 2.8 reveals other models' linearity: the ESDU model, ONERA model, and CFM56.

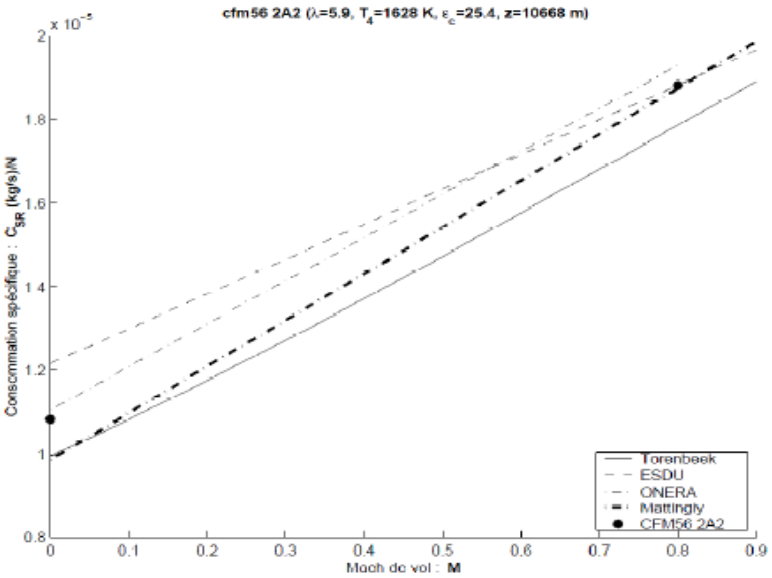

Figure 2.8 SFC as a function of Mach number for different calculation models (Bensel 2018)

According to Roux (2005), these models were not very precise, and their margin of error was 16% at a fixed point and 12% in the cruise phase.

Roux (2005) proposed another linear model, which is represented in (2.4). This model was identified from Torenbeek's (1997) model (2.3) then readjusted on experimental data of 60 engines and have an error of 6.05%.

$$SFC = \Big(\big(a_1(h)\cdot\lambda + a_2(h)\big)\cdot M + \big(b_1(h)\cdot\lambda + b_2(h)\big)\Big)\cdot\sqrt{\theta} + (7.4\cdot 10^{-13}(\varepsilon_c - 30)\cdot h + c)(\varepsilon_c - 30) \tag{2.4}$$

where

$$\theta = \frac{T(h)}{T_0}$$

h	Altitude (m)
M	Flight Mach Number
ε_c	Inlet/outlet pressure ratio of the compressor on the ground
λ	Bypass Ratio
a_1, a_2, b_1, b_2, c	Constants that depend on Altitude

Herrmann (2010) also proposed another calculation model based on engine performance analysis and build from Torenbeek (1997).

$$SFC = \frac{0{,}679 \cdot \sqrt{\frac{T(h)}{T_0}}\left(\phi - \mu - \frac{K}{\eta_c}\right)}{\sqrt{5\eta_n\left(1 + \eta_f\eta_t\lambda\right) \cdot \left(G + 0.2M^2\,\frac{\eta_c}{\eta_f\eta_t}\lambda\right)} - (1+\lambda)M} \tag{2.5}$$

In this equation, the flight altitude h has an indirect influence since it determines the temperature relationship between the altitude-dependent temperature and the ground temperature at sea level. The model stipulates that, corresponding parameters must be specified for each calculation of the thrust-specific consumption.

2.2.2 Models for Thrust Calculations

The development of a thrust calculation model is a necessary step in designing a turbojet engine. The existing engine thrust models are mainly based on the aerodynamic and thermodynamic analysis of the engine cycle. They are also suitable for particular flight phases. (Roux 2005)

The variation of thrust is mainly linked to height and velocity. Many authors have created thrust models based on one of the two factors to facilitate the calculations and reduce the error percentage.

- Effect of Velocity on Thrust

Mattingly (2002) proposed a thrust model for engines with a high dilution rate. The effect of the altitude on the decrease of Mach number is neglected.

$$\frac{F}{F_0} = \left(\frac{\rho(h)}{\rho_0}\right)^{0.6} (0.568 + 0.25\,(1.2 - M)^3) \tag{2.6}$$

where

F Maximum thrust in cruise phase (N)
F_0 Maximum thrust at a fixed point (N)
ρ Density of the air at $h \neq 0$ ($\mathrm{kg \cdot m^{-3}}$)
ρ_0 Density of the air at $h = 0$ ($\mathrm{kg \cdot m^{-3}}$)

Mattingly (2002) also proposed an algorithm allowing the resolution of complex models based on engine cycle study and considering engine parameters.

Roux (2005) mentioned another model to evaluate the loss of thrust during the take-off phase $F_{0_{max}}$ which is Torenbeek (1997) model. The author took in consideration the fact that, thrust and mass flow through the engine is constant over a speed range of up to Mach 0.2.

$$\frac{F}{F_0} = 1 - \frac{0.454(1-\lambda)}{\sqrt{(1+0.75\lambda)G}} M + \left(0.6 + \frac{0.13\lambda}{G}\right) M^2 \tag{2.7}$$

with

G Gas generator power function

λ Bypass ratio

Roux (2005) mentioned the ONERA model based on the engine cycle study, aerodynamic and thermodynamic laws to estimate a turbojet engine's thrust. The author mentioned that this model could determine a turbofan engine's behavior in any flight conditions, provided that at least the characteristics of a single cycle are known.

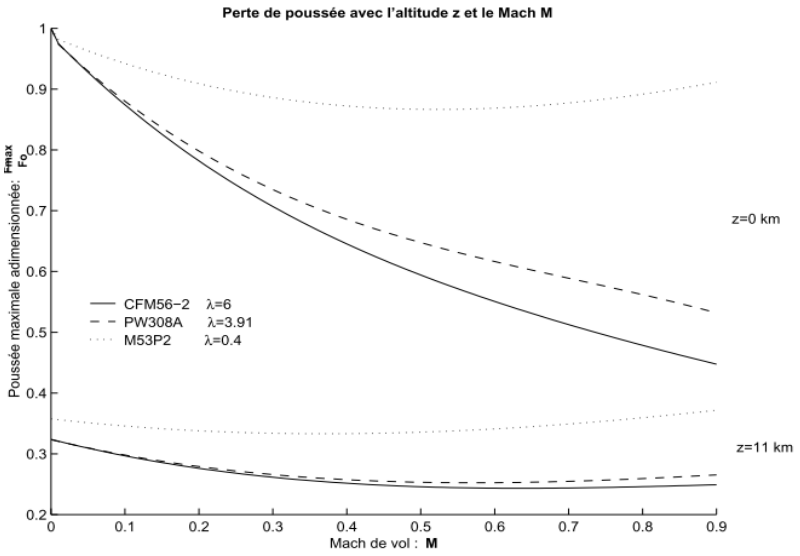

Figure 2.9 ONERA Simulation: Thrust loss as a function of Mach number and altitude for different engines (Roux 2005, page 48)

Bartel (2008) described Cruise thrust divided by thrust at sea level without considering the impact of bleed air extraction in

$$\frac{F}{F_0} = 1 - k_1 M + k_2 M^2 \quad , \tag{2.8}$$

with

k_1, k_2 factors related to fundamental engine design parameters

This basic model was first created to provide good accuracy for Mach numbers below 0.2. (2.8) was later developed by the authors to represent new aero-engines performance over a wider Mach number range.

$$\frac{F}{F_0} = 1 - \frac{0.377\ (1-\lambda)}{\sqrt{(1+0.82\lambda)\ G_0}}\ M + \left(0.23 + 0.19\sqrt{\lambda}\ \right) M^2 \qquad (2.9)$$

where

G_0 Gas generator power function at sea level

The authors used engine performance data to compare Torenbeek's model from (2.7) with their model from (2.9). Figure 2.10 shows that the model created by Bartel (2008) is more precise for a Mach number greater than 0.2, which proves the reduction in the margin of error.

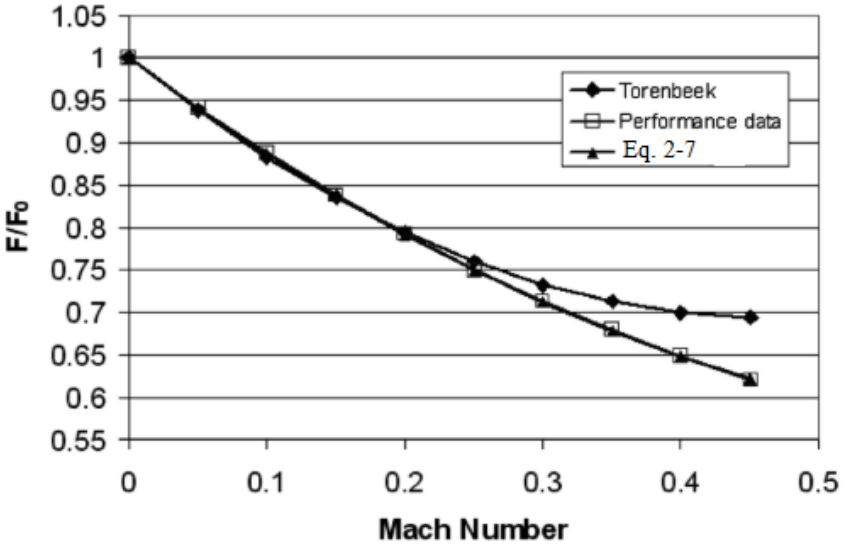

Figure 2.10 Difference between (2.8) and Torenbeek's approach from (2.6) (Bartel 2008, page 1453)

- Effect of Altitude on Thrust

For the investigation of thrust with altitude, many authors have proposed linear or simple polynomial models. Schulz (2007) mentioned a linear model represented in

$$\frac{F}{F_0} = \sigma^x \quad , \qquad (2.10)$$

where

F Maximum thrust in cruise phase (N)
F_0 Maximum thrust at a fixed point (N)
x Variable coefficient

As given by Scholz (2019a), (2.10) became

$$\frac{F}{F_0} = a \cdot \sigma^n \quad , \tag{2.11}$$

where

$a = -0.0253 \cdot \lambda + 0.7291$
$n = 0.0033 \cdot \lambda + 0.7324$

Ojha (1995) created a linear model to estimate thrust with height. The model created is represented in (2.12). The author explained that thrust decreases from sea level until 55000 ft.

$$\frac{F}{F_0} = 1 - C \cdot h \tag{2.12}$$

where

$C = -0.000018\ \text{ft}^{-1}$
h Height (ft)

As given by Scholz (2015), (2.13) is Another model describing the variation of cruise thrust and take-off thrust with the Bypass ratio and cruise altitude. This estimation is meant to be used for preliminary design.

$$\frac{F}{F_0} = (0.0013 \cdot \lambda - 0.0397) \cdot \left(\frac{1}{\text{km}}\right) \cdot h - 0.0248 \cdot \lambda + 0.7125 \tag{2.13}$$

- Effect of Altitude and Velocity on Thrust

Bartel (2008) extended (2.9) by including empirical factors, designed as A, Z, and X, dependent only on the relative air pressure. These factors are calculated from the engine data.

$$\frac{F}{F_0} = \text{A} - \frac{0.377\ (1+\lambda)}{\sqrt{1 + 0.82\ \lambda)\ G_0}}\ ZM + \left(0.23 + 0.19\sqrt{\lambda}\right) XM^2 \tag{2.14}$$

with

$$A = -0.4327 \left(\frac{P_{amb}}{P_{amb_0}}\right)^2 + 1.3855 \frac{P_{amb}}{P_{amb_0}} + 0.0472$$

$$Z = 0.9106\left(\frac{P_{amb}}{P_{amb_0}}\right)^3 - 1.7736\left(\frac{P_{amb}}{P_{amb_0}}\right)^2 + 1.8697\frac{P_{amb}}{P_{amb_0}}$$

$$X = 0.1377\left(\frac{P_{amb}}{P_{amb_0}}\right)^3 - 0.4374\left(\frac{P_{amb}}{P_{amb_0}}\right)^2 + 1.3003\frac{P_{amb}}{P_{amb_0}}$$

P_{amb} ambient pressure (Pa)
P_{amb_0} ambient pressure at sea level (Pa)

The authors confirmed that the results obtained from (2.9) and (2.13) are 1% better for the flight speeds up to Mach 0.4.

3 Analysis of Engine Parameters

In this chapter, the units presented in Table 3.1 must be respected to guarantee the correct results.

Table 3.1 Units of the parameters used in the equations

Parameters	Abbreviations	Units
Thrust	F	N
SFC	C	Kg/Ns
SFC factor	C_a	kg/Nm
SFC factor	C_b	kg/Ns
Cruise Altitude	H	m
Engine Mass	M	kg
Fan Diameter	D_{fan}	m
Engine Length	l_{eng}	m
Engine Diameter	D_{eng}	m
Engine Volume	V_{eng}	m^3
Temperature	T	K
Speed	V	m/s

3.1 Calculation of C_a and C_b from SFC and Cruise Mach Number

According to Meier 2005, the technical information gathered from the "Civil Turbojet/Turbofan Specifications" database is classified into three categories:

- Technical parameters on the ground contain the thrust on a wet and dry runway, SFC also on a wet and dry runway, Bypass ratio, etc.
- Technical parameters in the cruise phase are thrust, SFC, speed, and altitude.
- Conceptual engine parameters.

For the calculation of C_a and C_b, the model used is Mattingly's model, which was later adjusted by Roux (2005) and Scholz (2017) represented in (2.2).

3.1.1 Calculation of C_b

Since the aircraft produces thrust on the ground even when the speed is equal to zero, the value of the factor C_b is defined. Mathematically, from Figure 2.8, C_b is the intercept. In this case, if V is equal to zero, that means C_a times V is equal to zero and SFC_{grd} is equal to C_b.

Therefore, (2.2) becomes

$$SFC_{grd} = C_0 = C_b \quad . \tag{3.1}$$

According to Mattingly 1996, C_b depend on the height. This means that, if the altitude increases, the consumption in standing thrust also decreases. This will lower the entire straight line. Torenbeek's model which was proposed by Roux 2005 approves this theory. In Figure 1.6, it is shown that the more BPR increases, the more the slope of this line increases, while the intercept C_b decreases.

So according to Scholz (2017)

$$C_b = C_{b_0}\sqrt{\frac{T(h)}{T_0}} \quad , \tag{3.2}$$

where

C_{b_0} Specific fuel consumption at an altitude h equal to Zero (kg/Ns)
T Temperature for a given altitude (K)
T_0 Temperature at sea level (K)
h Altitude (m

3.1.2 Calculation of Temperature in Cruise Altitude

According to Anderson (1989), the atmosphere can be split into five layers as shown in Figure 3.1.

The temperature variation is not constant for all the layers. That is why the aircraft's maximum cruise altitude must be taken into consideration. This study will focus only on the troposphere and stratosphere, which are the maximum altitude accessible by commercial aircraft.

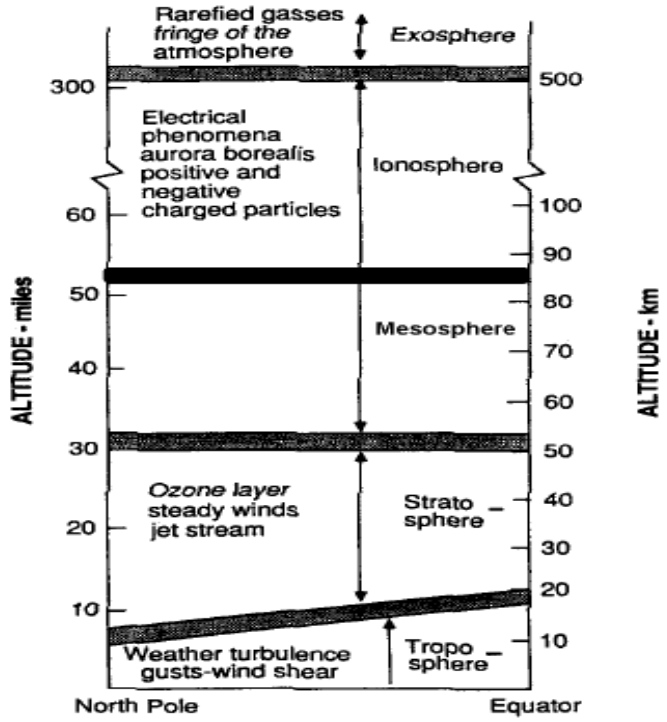

Figure 3.1 Basic classification of the atmosphere (Anderson 1989)

Figure 3.2 shows the temperature distribution in the standard atmosphere. In the troposphere (between 0 km and 11 km), the temperature varies linearly with the altitude.

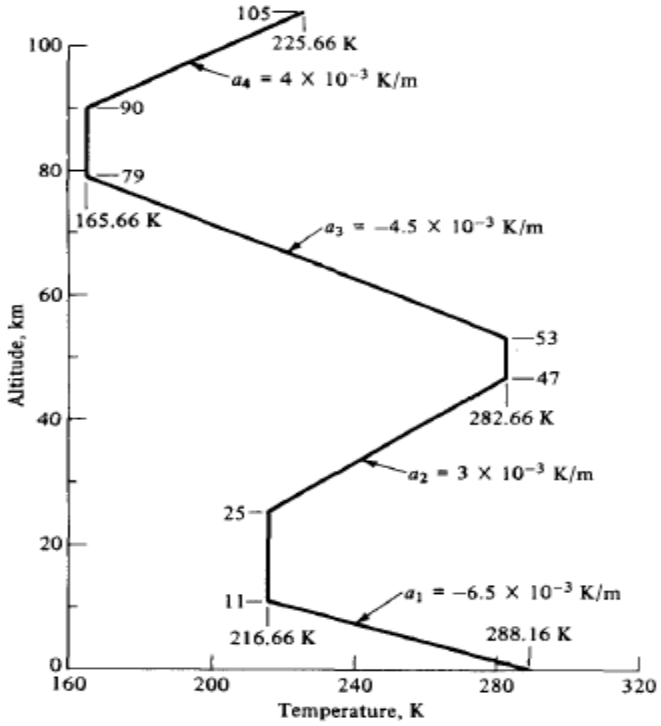

Figure 3.2 Temperature distribution in the standard atmosphere (Anderson 1989, page 117)

It can be explained by

$$T_{Cruise_{Tr}} = T_0 + a_1\, h \quad , \tag{3.3}$$

where

$T_{Cruise_{Tr}}$ Cruise temperature at the troposphere (K)

a_1 Adiabatic thermal gradient for the troposphere

From Figure 3.2, the standard temperature at sea level T_0 is 288.16 K, which is 15°C. Also, the constant adiabatic thermal gradient for the troposphere is a_1 equal to $-6.5 \cdot 10^{-3}$ K per m. This adiabatic thermal gradient is linear up to the tropopause, which is the upper limit of the troposphere where the temperature stops decreasing to reach an average value of 216.66 K in temperate regions.

At altitudes higher than the troposphere, the temperature is always modeled by a linear function, but its gradient takes other values.

In the stratosphere (between 11 km and 47 km), as shown in Figure 3.2, the temperature variation is constant between 11 km and 25 km, and it increases linearly from 25 km until 47 km. Since commercial aircrafts typically cruise altitudes are between 9 km and 12 km, our focus will be only on the lower reaches of the stratosphere.

$$T_{Cruise_{St}} = 216.66\ K = -56.5°C \tag{3.4}$$

Where

$T_{Cruise_{St}}$ Cruise temperature at the stratosphere (K)

3.1.3 Calculation of C_a

First, the speed must be written under another form. From Scholz (2017)

$$V = a\, M = a_0 \sqrt{\theta}\, M \quad . \tag{3.5}$$

With

$$\theta = \frac{T_{cruise}(h)}{T_0} \tag{3.6}$$

So, (3.5) in (2.2) becomes

$$SFC_{Cruise} = C_{T_{Cruise}} = C_a \, a_0 \sqrt{\frac{T_{Cruise}(h)}{T_0}} \, M + C_b \quad . \tag{3.7}$$

Based on (3.7), the temperature estimation and the estimation of C_b, C_a can now be deducted.

$$C_a = \frac{C_{T_{Cruise}} - C_b}{a_0 \sqrt{\frac{T_{Cruise}}{T_0}} \, M} \tag{3.8}$$

Where

a_0	Speed of sound m/s
M	Flight Mach number
T_{Cruise}	Cruise temperature (K)
T_0	Temperature at sea level (K)
C_T	Specific fuel consumption at cruise phase kg/(Ns) also known as SFC_{Cruise}

a_0 is the speed of sound, which is equal to 340 m/s at standard atmospheric conditions ($T_0 = 15°\text{C}$ and $P_0 = 1013{,}25$ hPa).

The value of C_a can be deduced now that all the parameters have been calculated. (3.8) is applied for all engines mentioned in the database created by Meier (2005). The calculation part was carried out and assembled in an Excel spreadsheet.

3.2 Extraction of C_a and C_b from an Engine Database and Correlation

3.2.1 Extraction of C_a and C_b for the Available Engine Models

The table created by Meier (2005) is an open-source database containing most of the existing turbojet engines as well as their operating and performance parameters. However, many parameters are still missing. That is why our first task was to collect as many parameters as possible to obtain better results. Of course, we do not pretend to present exact data without errors.

The first source was Roux (2007a). In her book, she has collected recent engine data listed under the engines' names. She had tried to compare the sources to make these data as reliable as possible.

Roux (2007b) is another source used to fill the engine parameters database. In this source, the author presented data for civil transport aircraft that she could find freely on the internet or in reference books.

DGAC (2020) is another source used to define the BPR of some of the existing engines. This database contains the ICAO noise database for most of the recent engines. It was validated by trusted sources like EASA, FAA, TCA, etc. We only took the BPR value to fill our database engine parameters paper.

Besides, Jenkinson (2001) is also a reliable source based on Jenkinson (1999). It is a database containing technical and operational data on current and projected engines from engine manufacturers, compiled from brochures and other published information.

Also, Bose (2012) proposed a database for airbreathing engine parameters used as a source for our research.

Another reliable source is Svoboda (2000). The author assembled engine data and plotted it mostly as a function of take-off thrust to define if an existing engine can be used in the proposed airplane.

Likewise, many parameters are still unknown. For this, an Excel code (Scholz 2019b) was used to estimate some values. These values are not 100% exact due to the lack of input parameters. This code can estimate the TSFC during the cruise phase if the input parameters are known.

We have tried to compare the sources to make these data as reliable as possible. However, the database is still not fully completed. Many values are still unknown and cannot be found on open sources. Hence the reason why the main focus will be on the available values.

The second step is to change the units of measurement from the Imperial system of units to the International System (SI-units).

Table 3.2 Unit change made on the gathered parameters

The imperial system of units	S.I unit
ft	0.3048 m
lb	0.4536 kg
lbf	4.44822 N
$\frac{\text{lb}}{\text{lbf} \cdot \text{h}}$	$0.283 \cdot 10^{-4} \frac{\text{kg}}{\text{N} \cdot \text{s}}$

The third step consists of calculating the cruise temperature using (3.3). The temperature at sea level is equal to 288.5 K, and the adiabatic thermal gradient is also constant and equal to -6.5 K per km for the troposphere. Regarding aircraft that have a flight level above the tropopause, the lower reaches of the stratosphere, the temperature is equal to 216.66 K.

In the next step, (3.2) is applied to calculate C_b. The values of SFC_{grd} are given in Meier (2005). Since either the dry or wet runway ground Specific fuel consumption value is available, the one that is given is chosen. After that, C_a is calculated using (3.8).

3.2.2 Correlation of C_a and C_b with BPR and Date of Entry into Service

The specific fuel consumption depends on a variety of factors. To study the variation of C_a and C_b, the Mach number and the altitude in cruise phase need to be constant. Due to the lack of data, our choice was fixed on engines with 0.8 cruise Mach number and 35000 ft cruise altitude.

3.2.2.1 Variation of C_a and C_b with BPR

The relationship between SFC and BPR was plotted from the engine data for both take-off and cruise phases, as shown in Figure 3.3 and Figure 3.4.

The shape of the trend curve decreases as expected and proved by Svoboda (2000) and Dankanich (2017)**.** However, it is noticeable that many data points lie out of the trend curve, which can be explained by the fact that all plotted engines are not recent designs, which

means that engines designed in the twentieth century may not be as efficient as engines designed in the twenty-first century. Moreover, SFC is affected by other design parameters like engine mass, maximum thrust etc.

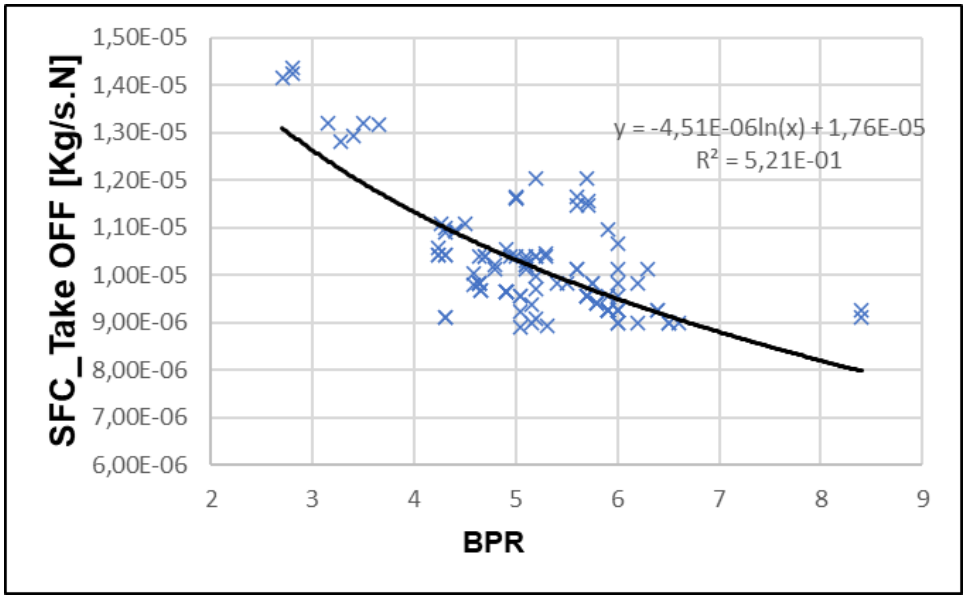

Figure 3.3 Bypass ratio effect on take-off specific fuel consumption

$$C_0 = -4{,}51 \cdot 10^{-6}\ \ln(\lambda) + 1{,}76 \cdot 10^{-5} \tag{3.9}$$

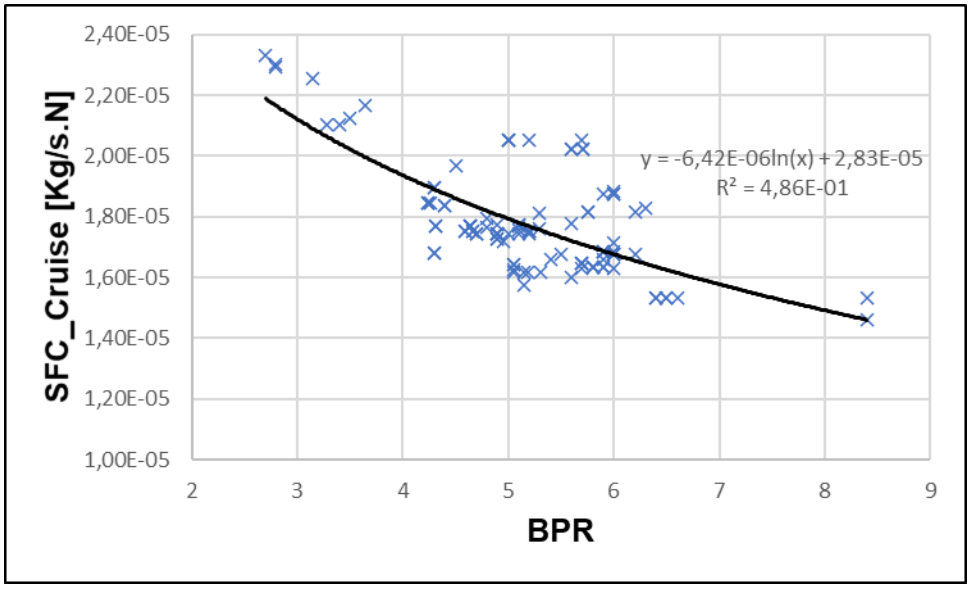

Figure 3.4 Bypass ratio effect on cruise specific fuel consumption

$$C_t = -6{,}42 \cdot 10^{-6}\ \ln(\lambda) + 2{,}83 \cdot 10^{-5} \tag{3.10}$$

Then, the values of C_a and C_b are plotted as a function of BPR in a scatter graphic. Afterward, several types of regressions were tested to adjust the coefficient of determination R^2. Next, a

logarithmic trend curve was plotted to clarify the variation of C_a and C_b as shown in Figure 3.5 and Figure 3.6.

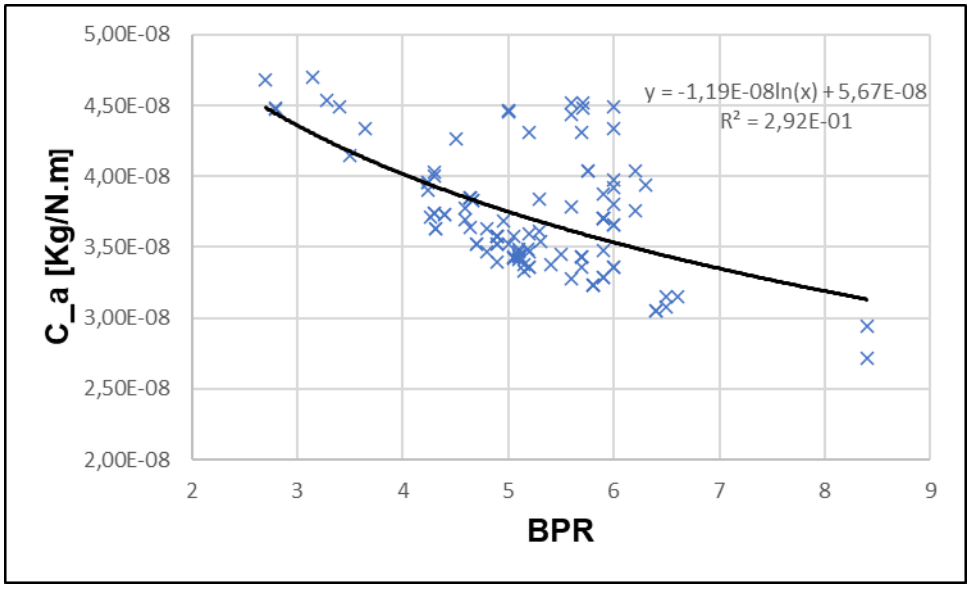

Figure 3.5 Variation of C_a with Bypass ratio

$$C_a = -1{,}19 \cdot 10^{-8}\ \ln(\lambda) + 5{,}67 \cdot 10^{-8} \tag{3.11}$$

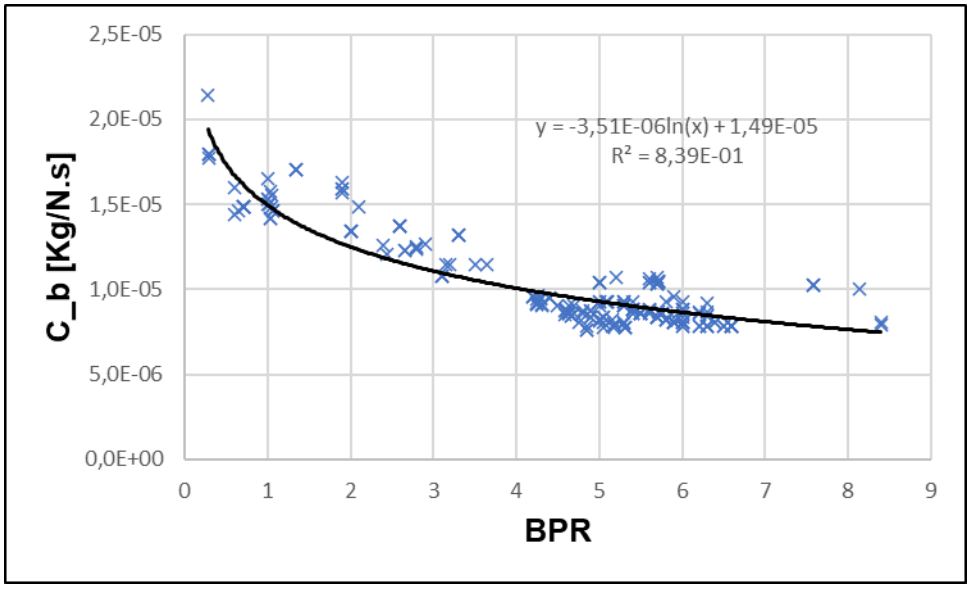

Figure 3.6 Variation of C_b with Bypass ratio

$$C_b = -3{,}51 \cdot 10^{-6}\ \ln(\lambda) + 1{,}49 \cdot 10^{-5} \tag{3.12}$$

In Figure 3.5, the value of R^2 is 0.29, which is low. That means, only 29% of C_a is predicted from BPR. This is due to the dependency of C_a on other parameters. Unlike C_a, the value of R^2 for C_b is 0.84, which is exceedingly high and indicates a great fit. That means, the model describing C_b as a function of BPR is a reliable model for future forecasts.

The trend curve shows that both C_a and C_b decreases by increasing the bypass ratio.

From (2.2) and the results obtained from Figure 3.4, Figure 3.5, and Figure 3.6, we can conclude that BPR affects mostly C_b which acts on the rate of variation of SFC.

3.2.2.2 Variation of C_a and C_b with Entry into Service Date

During the last 100 years, jet engines have been improved in a variety of ways. One of the most important upgrades has been made to reduce specific fuel consumption. This Amelioration is vital for commercial airlines which rely on the turbofan engine to deliver high efficiency and high thrust to carry people across the globe and at the same time to make profits.

Figure 3.7 and Figure 3.8 show the variation of specific fuel consumption between 1950 and 2012.

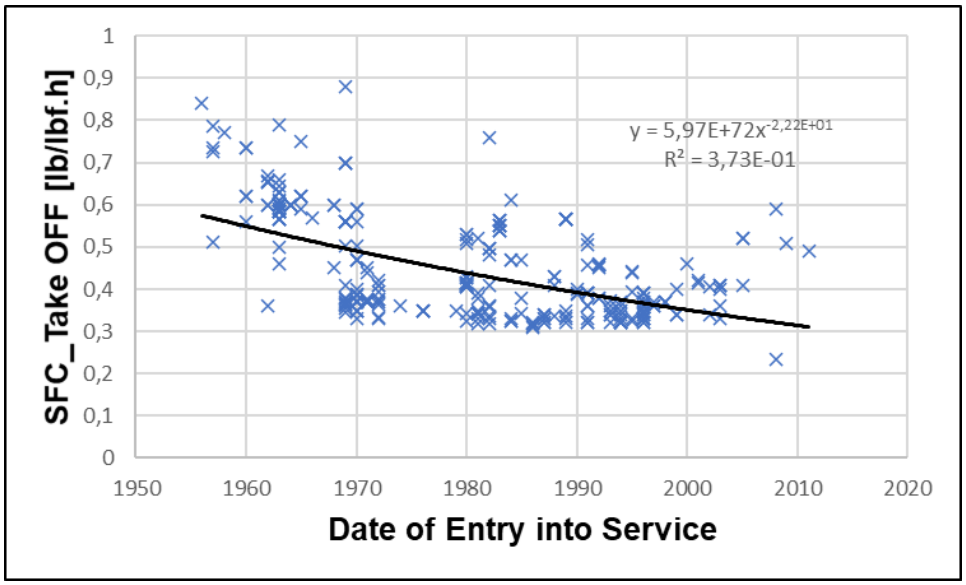

Figure 3.7 Take-off Specific fuel consumption variation over time

$$C_0 = 5{,}97 \cdot 10^{72} \cdot t^{-22{,}2} \tag{3.13}$$

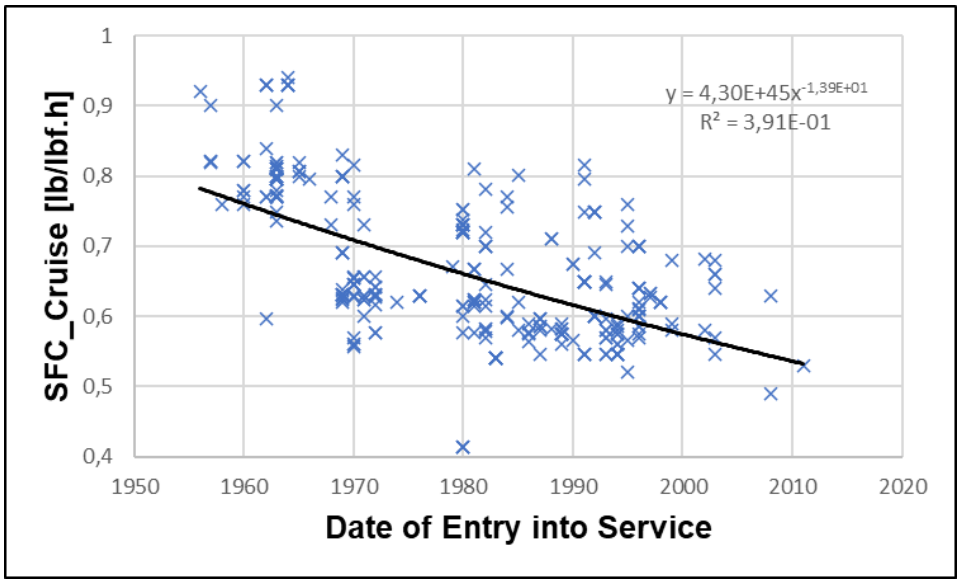

Figure 3.8 Cruise Specific fuel consumption variation over time

The trend of the curve decreases with time as expected which explains the evolution of turbojet engines.

$$C_t = 4{,}30 \cdot 10^{45} \cdot t^{-13{,}9} \tag{3.14}$$

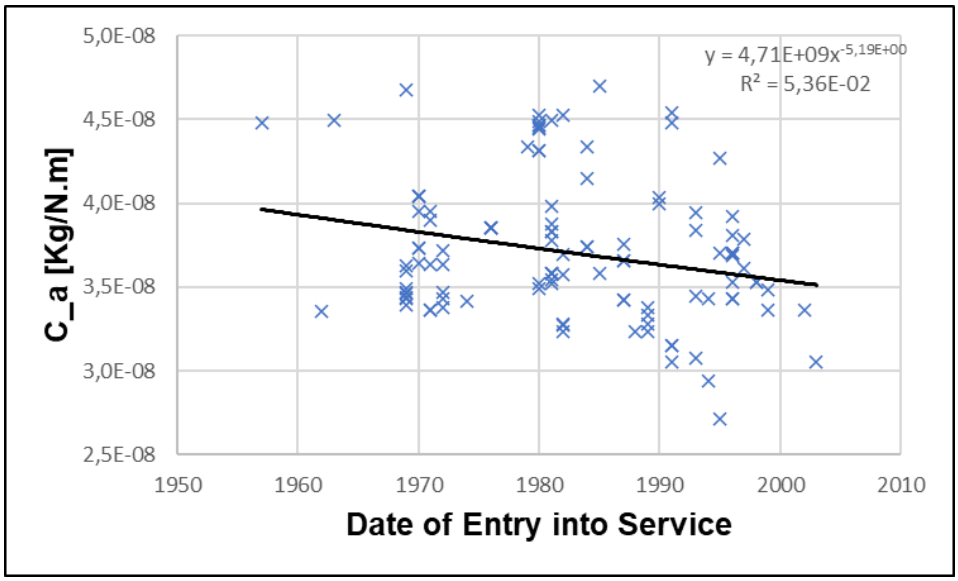

Figure 3.9 Variation of C_a over time

$$C_a = 4{,}71 \cdot 10^{9} \cdot t^{-5{,}19} \tag{3.15}$$

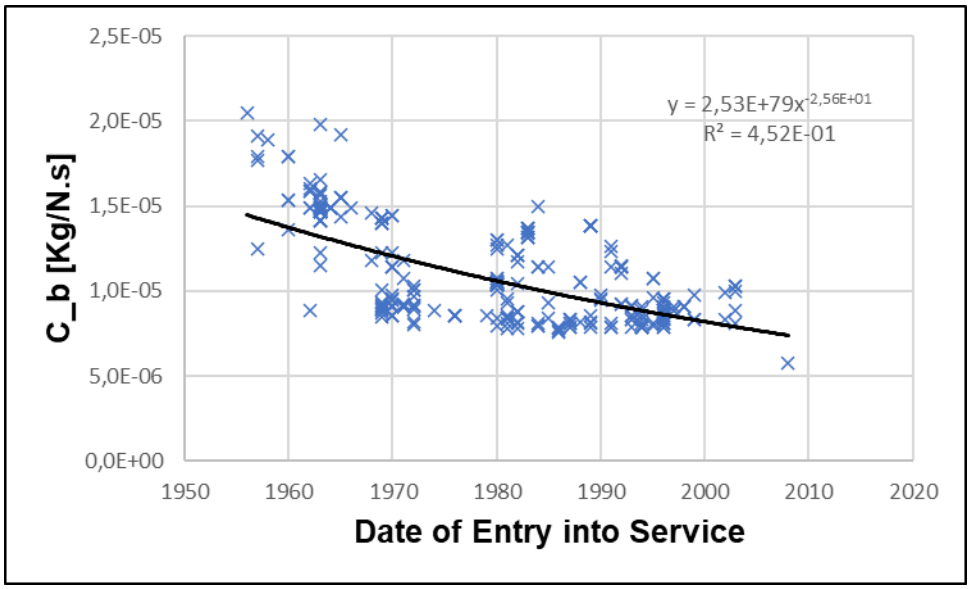

Figure 3.10 Variation of C_b over time

$$C_b = 2{,}53 \cdot 10^{79} \cdot t^{-25{,}6} \tag{3.16}$$

In Figure 3.9 and Figure 3.10, C_a and C_b are plotted over time. The look of both curves is similar to Figures 3.5 and 3.6. This can be explained by the fact that BPR increases over time. Figure 3.11 shows this variation.

The BPR is a crucial parameter acting directly on the SFC reduction. The improvements made on BPR are very noticeable from Figure 3.11.

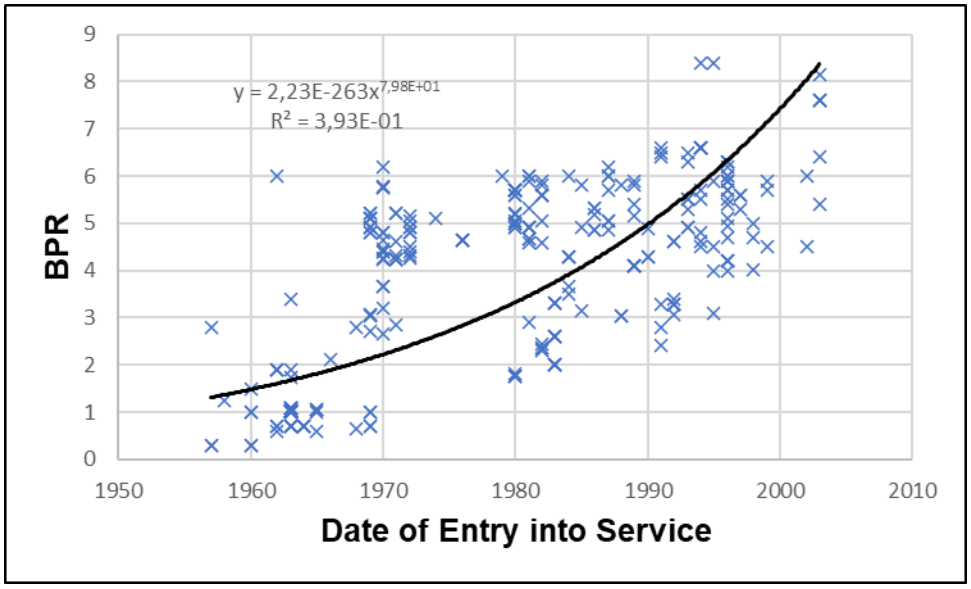

Figure 3.11 Variation of Bypass ratio over time

$$\lambda = 2{,}23 \cdot 10^{-263} \cdot t^{79{,}8} \tag{3.17}$$

However, the data in our possession is limited. We cannot analyze the turbofan engines' improvement during the last years due to the lack of data.

3.2.3 Engine Mass Dependency on Thrust, BPR, and Engine Geometric Parameters

3.2.3.1 Variation of Engine Mass with Thrust

In Figure 3.12 and Figure 3.13, engine mass is plotted as a function of take-off and cruise thrust.

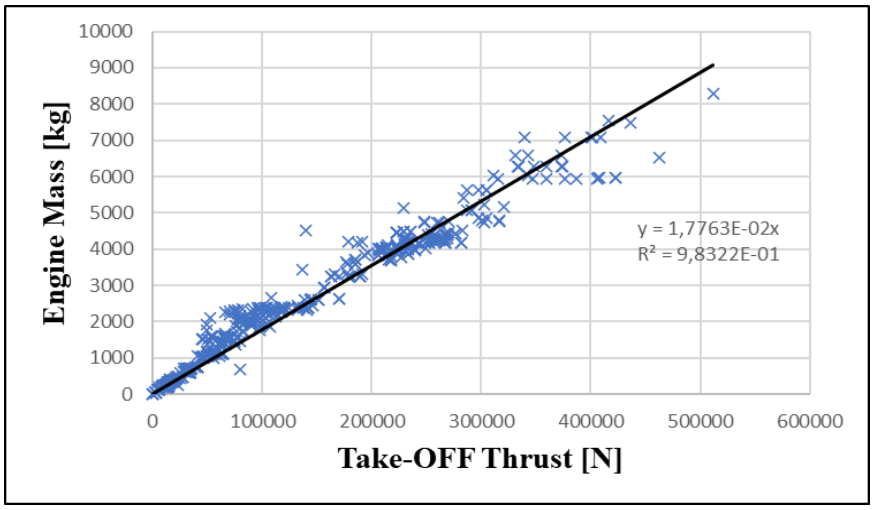

Figure 3.12 Engine Mass as function of Take-off Thrust

$$m = 1{,}776 \cdot 10^{-2}\, T_0 \tag{3.18}$$

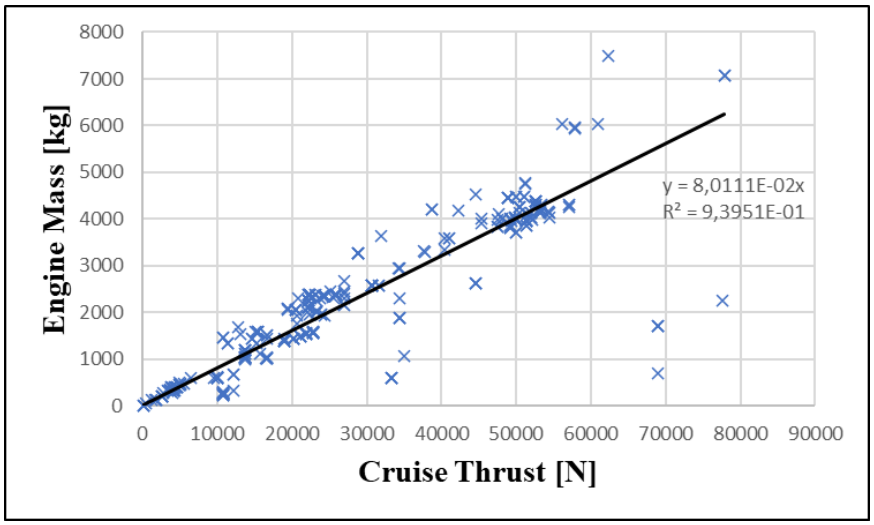

Figure 3.13 Engine Mass as function of Cruise Thrust

$$m = 8{,}011 \cdot 10^{-2}\, T_c \tag{3.19}$$

It must be understood that many currently produced engines have a de-rated take-off thrust to extend engine life. It is also essential to understand that most of the engines plotted are still in production, and many are not recent designs. Also, the bypass ratio of these engines varies between 0 and 9 during the cruise phase. This can affect the linearity of the trend. That means some engines can appear to be either above or under the trend. The determination coefficient is remarkably high, proving that the relationship between engine mass and thrust for both flight phases is linear and nearly fits.

3.2.3.2 Variation of Engine Mass with BPR

Figure 3.14 shows the relationship between Engine Mass and Bypass ratio.

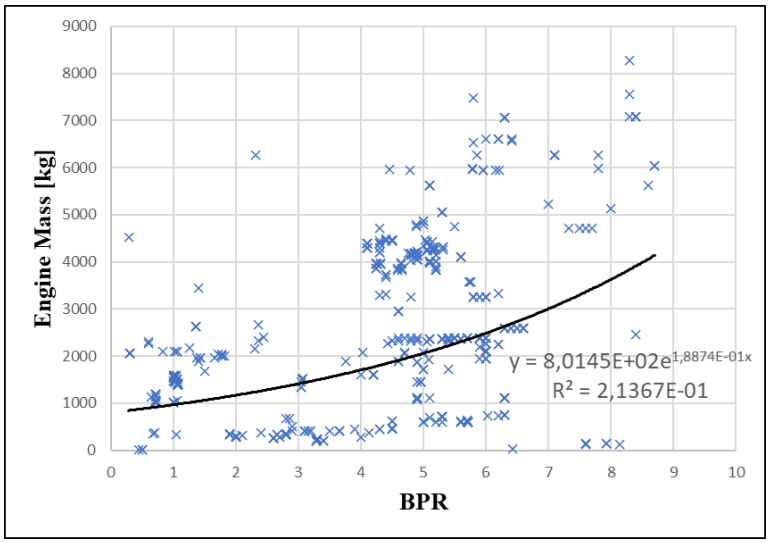

Figure 3.14 Engine Mass as function of Bypass ratio

$$m = 8{,}05 \cdot 10^{2} e^{1{,}887 \cdot 10^{-1} \cdot \lambda} \tag{3.20}$$

Many engines seem not to be on the trend curve. The engine's mass depends on geometric parameters like length, fan diameter, Nacelle diameter, number of spools, etc. Some of those parameters are arbitrary design choices and are not similar for all engines, which creates this large amount of scattering.

Likewise, BPR is a vital function of the type of application and an arbitrary design choice that needs to be investigated during the design phase.

The BPR increases the thrust of a turbojet engine, leading to an increase in Mach number. At the same time, the increase in BPR reduces the specific fuel consumption. However, it is essential to remember that BPR and dry mass act proportionally, which means, to increase the

BPR, the fan's size needs to be increased, leading to a mass increase. Furthermore, by increasing the mass, the specific fuel consumption will also increase.

That is why the right choice of parameters is essential to balance the turbojet engine's dry weight, the BPR, and thrust by reducing the SFC as much as possible.

3.2.3.3 Variation of Engine Mass with Engine Geometric Parameters

In Figure 3.15, the engine's dry mass was plotted as a function of the fan diameter. It is expected that by increasing the fan's size, the engine's mass will also increase linearly.

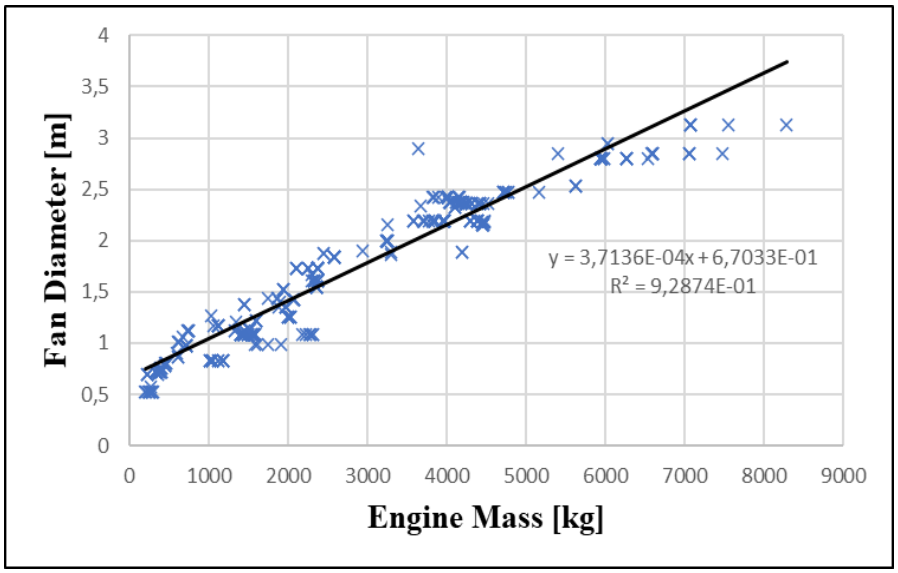

Figure 3.15 Variation of Engine Mass with Fan Diameter

$$D_{fan} = 3{,}714 \cdot 10^{-4}\, m + 6{,}703 \cdot 10^{-1} \tag{3.21}$$

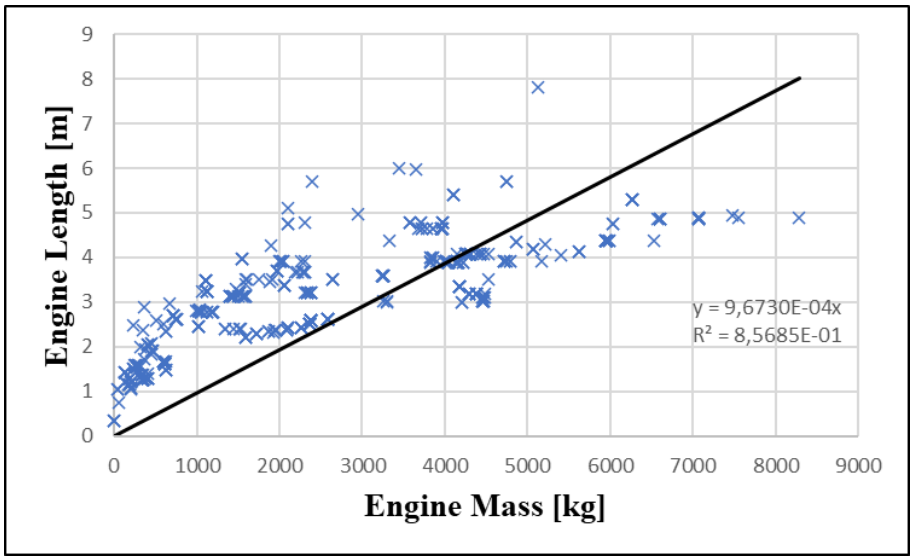

Figure 3.16 Variation of Engine Mass with Engine Length

$$l_{eng} = 9{,}673 \cdot 10^{-4}\, m \tag{3.22}$$

Same for Figure 3.16 and Figure 3.17, the engine mass was plotted as a function of engine length and engine diameter.

The geometric parameters of engines are an important design choice. They act directly on the specific fuel consumption and the thrust produced. It is known that, by increasing the size of the fan, the BPR will be increased, which produces more thrust. However, the Fan size increase leads to an increase in the engine mass, which engenders more fuel consumption during take-off and cruise phases.

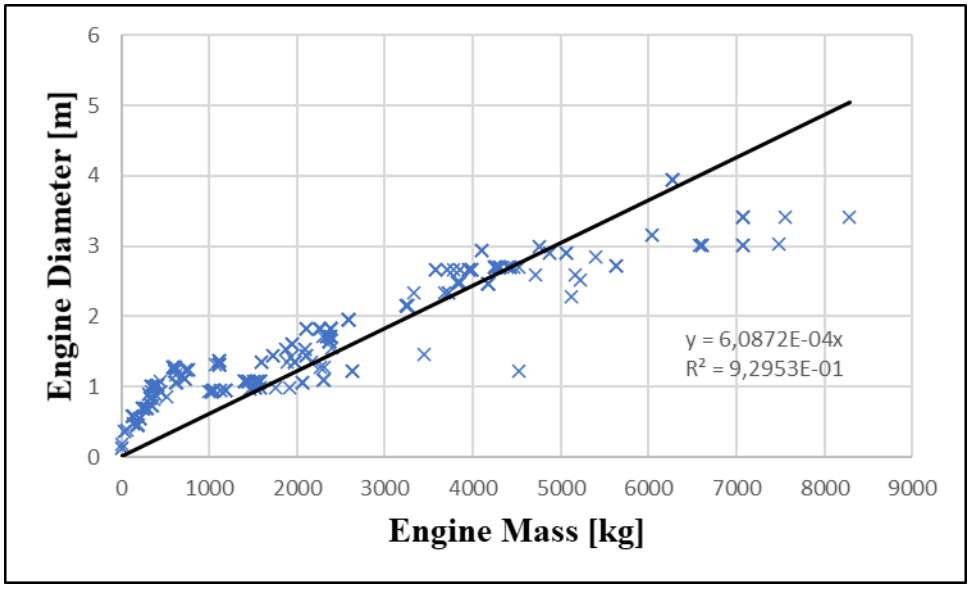

Figure 3.17 Variation of Engine Mass with Engine Diameter

$$D_{eng} = 6{,}087 \cdot 10^{-4}\, m \tag{3.23}$$

Assuming now that the engine is a perfect cylinder. The volume of the turbojet engine was first calculated using

$$Volume = \frac{\pi}{4} \times Diameter^2 \times Length \ . \tag{3.24}$$

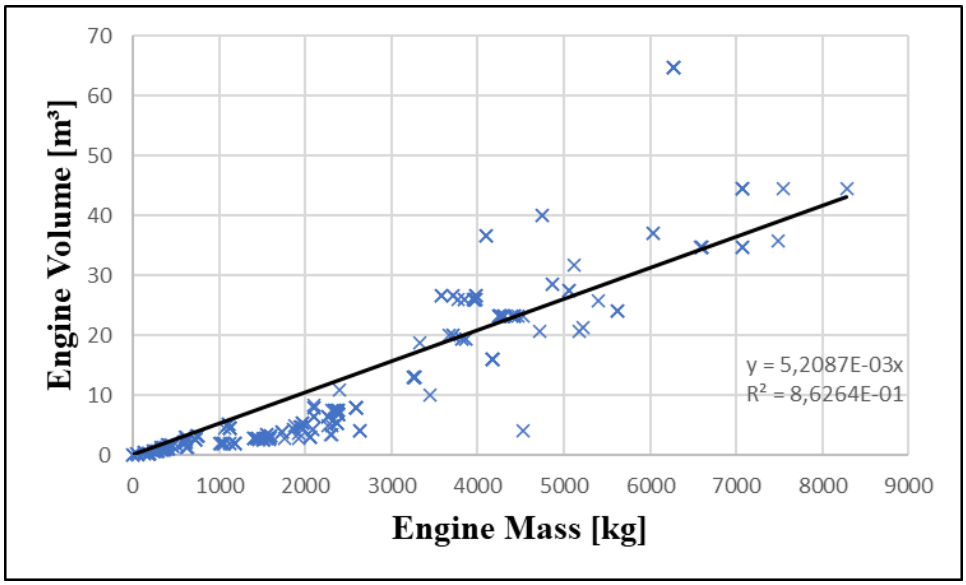

Figure 3.18 Variation of Engine Mass with Engine Volume

$$V_{eng} = 5{,}209 \cdot 10^{-3}\, m \tag{3.25}$$

In Figure 3.18, the estimated volume of each available engine was plotted as a function of engine mass. The trend of the curve obtained is a linear equation with a coefficient of determination R^2 equal to 85%. This coefficient is high enough to prove that this model is highly reliable for future forecasts.

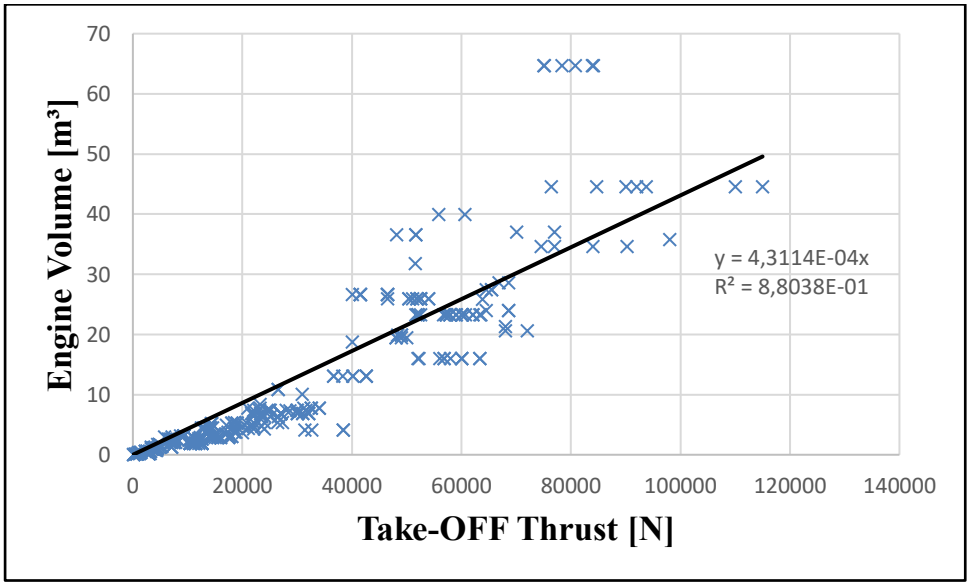

Figure 3.19 Variation of Take-off Thrust with Engine Volume

$$V_{eng} = 4{,}3114 \cdot 10^{-4}\, T_o \tag{3.26}$$

Because of the linearity of engine mass with take-off thrust and with engine volume, the variation of take-off thrust and engine volume is also a linear function as shown in Figure 3.19.

By Increasing the volume of a turbojet engine, many other design parameters are improved. The number of spools can be quoted as a good example. Also, the increase of compressor and turbine stages can boost the thrust. However, the engine will be heavier, and the SFC will increased.

In this analysis, the type of materials is not considered. Many recent design engines use modern alloy materials such as titanium, nickel, and aluminum alloys even though their significant volume. Those materials provide high strength to mass ratio, which is essential for the design of an engine.

3.3 New Equations for SFC

The objectives of model identification are to estimate the engine performances during the design phase, predict and represent their behavior during all flight phases, and facilitate decision-making during aircraft manufacturing stages. Most existing models are based on either linear equations or polynomial equations. These analytical models allowed the estimation of engine parameters while ensuring the high quality of its performance and precision.

3.3.1 SFC Models from Linear Regression

To build a specific fuel consumption model, the relationship between design parameters has been investigated based on the database from Meier (2005) using a multilinear regression on excel.

In the first model, the specific fuel consumption was the dependent variable. Thrust, cruise altitude, Mach number, BPR, and engine mass were the independent variables. This relationship is explained in

$$SFC_{Cruise} = \beta_{21,0} + \beta_{22,1} \cdot F_{Cruise} + \beta_{22,2} \cdot h + \beta_{22,3} \cdot M + \beta_{22,4} \cdot \lambda + \beta_{22,5} \cdot m \quad , \quad (3.27)$$

where

$\beta_{22,i}$ Coefficient of the independent variables ($i = 0:5$)

m Engine Mass (kg)

Table 3.3 Summary output of the first SFC model (3.27)

Parameters	Coefficients	P-Values	R^2	Significant F
Intercept	$1{,}5 \cdot 10^{-5}$	$1{,}5 \cdot 10^{-9}$		
Thrust [N]	$1{,}6 \cdot 10^{-11}$	0,06		
Cruise Altitude [m]	$-4{,}2 \cdot 10^{-10}$	$3{,}5 \cdot 10^{-28}$	0,672	$1{,}54 \cdot 10^{-80}$
Mach Number	$2{,}97 \cdot 10^{-5}$	$1{,}06 \cdot 10^{-15}$		
BPR	$-6{,}86 \cdot 10^{-7}$	$5{,}08 \cdot 10^{-19}$		
Dry Mass [kg]	$-1{,}3 \cdot 10^{-9}$	$1{,}1 \cdot 10^{-17}$		

Table 3.3 is the result of the first regression. Approximately 67% of the variation in Specific fuel consumption is explained by thrust, Cruise altitude, Mach number, BPR, and Engine mass which is acceptable since the specific fuel consumption also depends on other parameters.

However, according to Mcleod (2019), a P-value higher than 0.05 is not statistically significant and fails to reject the null hypothesis. In this model, not all P-values for all the independent variables are less than 0.05, which means that not all the coefficients are statistically significant. The P-value of thrust is equal to 0.06, which concludes that there is no significant relationship between specific fuel consumption and thrust for this model.

In the second model, the thrust was excluded from (3.27), as shown in

$$SFC_{Cruise} = \beta_{23,0} + \beta_{23,1} \cdot h + \beta_{23,2} \cdot M + \beta_{23,3} \cdot \lambda + \beta_{23,4} \cdot m \quad , \tag{3.28}$$

where

$\beta_{23,i}$ Coefficient of the independent variables ($i = 0{:}\,4$)

Table 3.4 contains the results of the second regression. The value of R^2 is almost the same as the first model (67%). The significant F is equal to $6.23 \cdot 10^{-81}$ which is almost zero. Moreover, the P-values for all independent variables are less than 0.05. Additionally, the confidence interval does not include a zero. Therefore, the null hypothesis is rejected, and it is clear to say that the coefficients are statistically significant.

Table 3.4 Summary output of the second SFC model (3.29)

Parameters	Coefficients	P-Values	R^2	Significant F
Intercept	$1{,}48 \cdot 10^{-5}$	$2{,}44 \cdot 10^{-9}$		
Cruise Altitude [m]	$-4{,}13 \cdot 10^{-10}$	$1{,}65 \cdot 10^{-27}$		
Mach Number	$2{,}96 \cdot 10^{-5}$	$1{,}62 \cdot 10^{-15}$	0,67	$6{,}23 \cdot 10^{-81}$
BPR	$-6{,}82 \cdot 10^{-7}$	$9{,}28 \cdot 10^{-19}$		
Dry Mass [kg]	$-1{,}11 \cdot 10^{-9}$	$1{,}9 \cdot 10^{-22}$		

Therefore, the second model given in (3.29) is statistically significant with a smaller error percentage equal to 7.86% than the first model.

$$SFC_{Cruise} = 1.48 \cdot 10^{-5} - 4.13 \cdot 10^{-10} \cdot h + 2.96 \cdot 10^{-5} \cdot M - 6.82 \cdot 10^{-7} \cdot \lambda - 1.11 \cdot 10^{-9} \cdot m \quad (3.29)$$

Another linear model is presented based on (2.4). This model represents the specific fuel consumption as a function of overall pressure ratio, cruise thrust, BPR, Mach number, altitude, and mass.

Table 3.5 Summary output of the third SFC model (3.30)

Parameters	Coefficients	P-Values	R^2	Significant F
Intercept	$2{,}207 \cdot 10^{-5}$	$4{,}34 \cdot 10^{-16}$		
OPR at sea level	$-8{,}83 \cdot 10^{-8}$	0,0002		
Cruise Altitude [m]	$-4{,}94 \cdot 10^{-10}$	0,0003		
Mach Number	$1{,}02 \cdot 10^{-5}$	0,015	0,7	$5{,}88 \cdot 10^{-60}$
BPR	$-7{,}97 \cdot 10^{-7}$	$2{,}68 \cdot 10^{-21}$		
Dry Mass [kg]	$-5{,}7 \cdot 10^{-10}$	0,00013		
Thrust [N]	$1{,}59 \cdot 10^{-11}$	0,027		

$$SFC_{Cruise} = 1.59 \cdot 10^{-11} \cdot F_{Cruise} - 4.94 \cdot 10^{-10} \cdot h + 1.02 \cdot 10^{-5} \cdot M - 7.97 \cdot 10^{-7} \cdot \lambda - 5.7 \cdot 10^{-10} \cdot m - 8.83 \cdot 10^{-8} \cdot \varepsilon_c + 2.207 \cdot 10^{-5} \quad (3.30)$$

The coefficient of determination R^2 for this model is equal to 70%, as shown in Table 3.5. This model is also significant as the previous one. However, it includes two more parameters that allow it to be more interesting. The P-values for all independent variables are less than 0.05, which means that the null hypothesis is rejected. Likewise, the error percentage is equal to 5.28%, which is better than the previous model.

The fourth model represented in (3.31) is created based on (2.2), which describe the relationship between specific fuel consumption and speed by including the coefficients C_a and C_b.

Table 3.6 Summary output of the fourth SFC model (3.31)

Parameters	Coefficients	P-Values	R^2	Significant F
Intercept	$7{,}7 \cdot 10^{-6}$	0,016	0,03	0,0006
Velocity [m/s]	$4{,}68 \cdot 10^{-8}$	0,0006		

Although only 3% of the variation in Specific fuel consumption is explained by speed, this model is significant. The error margin is 14.7% which is relatively little for a preliminary design of an aircraft.

$$SFC_{Cruise} = 4.68 \cdot 10^{-8}\, V + 7.71 \cdot 10^{-6} \tag{3.31}$$

Conclusively, the third model fits the best as a linear model representing the specific fuel consumption as a function of other aircraft parameters.

3.3.2 SFC Models from Minimum Mean Square Error

The Minimum Mean Square is a procedure to determine the best fit line to data. The basic problem is to find the relationship between y and x based on the linear equation $y = ax + b$. However, the function y does not need to be linear. Several approaches can be considered in order to use statistics as a starting point for creating a calculation model.

First, the preliminary design parameters which are take-off thrust, cruise thrust, take-off SFC, OPR, and BPR are used to calculate an estimated value of C_a and C_b. Then, the sum of the squares from the difference between the real values and the estimated ones is calculated as shown in

$$\sum_{i=1}^{n} (y_i - \hat{y}_i)^2 \rightarrow 0 \ , \tag{3.32}$$

where

y_i Real values of C_a and C_b

$\hat{y}_i$ Estimated values of C_a and C_b

Afterward, the excel solver is used to determine the factors of the equations so that the deviations of both C_a and C_b are minimized compared to the statistical values of the respective aircraft model. Thus, the target cell of the solver is the sum of the squares from the difference between the calculated and actual values of C_a and C_b, the changing variables are the factors, and the solving method is "GRG Nonlinear". In the end, the sum of the differences is minimized, and the factors given by the solver represent the best values describing the relationship between the parameters for determining C_a and C_b. The results are represented in the Excel file "Error Least Square".

$$C_a = 3{,}96 \cdot 10^{-8} \cdot C_0^{5{,}3 \cdot 10^{-3}} \tag{3.33}$$

R^2	Err [%]
0,54	8,84

$$C_a = 9{,}594 \cdot 10^{-8} \cdot \lambda^{-0{,}6} \tag{3.34}$$

R^2	Err [%]
0,3	7,88

$$C_a = 9{,}5 \cdot 10^{-1} \cdot \lambda^{0{,}9} \cdot C_0^{1{,}6} \tag{3.35}$$

R^2	Err [%]
0,07	12,04

$$C_a = 9{,}5 \cdot 10^{-1} \cdot T_c^{0{,}2} \cdot C_0^{1{,}7} \tag{3.36}$$

R^2	Err [%]
0,04	13,42

$$C_a = 9{,}3 \cdot 10^{-1} \cdot \lambda^{0{,}9} \cdot T_c^{0{,}26} \cdot C_0^{1{,}8} \tag{3.37}$$

R^2	Err [%]
0,12	57,2

$$C_a = 5 \cdot 10^{8} \cdot T_0^{-0{,}6} \cdot T_c^{-0{,}4} \cdot \lambda^{0{,}77} \cdot C_0^{2{,}5} \tag{3.38}$$

R^2	Err [%]
0,43	78,7

The previous equations represent examples of the nonlinear models of C_a and the following ones are for C_b.

$$C_b = 7{,}46 \cdot 10^{-5} \cdot T_0^{-0{,}2} \tag{3.39}$$

R^2	Err [%]
0,65	11,37

$$C_b = 5{,}47 \cdot 10^{-5} \cdot T_{Cruise}^{-0{,}2} \tag{3.40}$$

R^2	Err [%]
0,51	12,18

$$C_b = 1{,}65 \cdot 10^{-5} \cdot \lambda^{-0{,}4} \tag{3.41}$$

R^2	Err [%]
0,5	5,81

$$C_b = 9{,}94 \cdot 10^{-6} \cdot \lambda^{8{,}37 \cdot 10^{-6}} \cdot T_{Cruise}^{1{,}25 \cdot 10^{-5}} \cdot T_0^{2{,}15 \cdot 10^{-5}} \tag{3.42}$$

R^2	Err [%]
0,58	15,63

$$C_b = 1{,}055 \cdot 10^{-5} \cdot \lambda^{-0{,}12} \cdot T_{Cruise}^{-0{,}7} \cdot T_0^{-0{,}8} \cdot C_0^{0{,}1} \tag{3.43}$$

R^2	Err [%]
0,6	6,23

Thereafter, the best calculation model is chosen based on the lowest percentage of error and the highest coefficient of determination R^2. To be specific, (3.33) is the best fitting model for C_a and (3.41) is the best one for C_b.

Finally, the specific fuel consumption during cruise phase is calculated from C_a and C_b models as shown in (3.44). Eventually, the percentage of error between the real SFC and the estimated SFC during cruise phase is determined.

$$C_{Cruise} = 3{,}96 \cdot 10^{-8} \cdot C_0^{5{,}3 \cdot 10^{-3}} \cdot V + 1{,}65 \cdot 10^{-5} \cdot \lambda^{-0{,}4} \tag{3.44}$$

R^2	Err [%]
0,23	6,16

The number of required parameters in (3.44) can be reduced to one. It has also been proven from (3.1) that $C_b = C_0$. That means (3.41) becomes

$$C_b = C_0 = 1{,}65 \cdot 10^{-5} \cdot \lambda^{-0{,}4} \quad . \tag{3.45}$$

Then, (3.45) will be replaced in (3.33) to obtain

$$C_a = 3{,}96 \cdot 10^{-8} \cdot (1{,}65 \cdot 10^{-5} \cdot \lambda^{-0{,}4})^{5{,}3 \cdot 10^{-3}} \quad . \tag{3.46}$$

Afterward, we replace C_a and C_b in (3.44) and obtain

$$C_{Cruise} = 3{,}735 \cdot 10^{-8} \cdot \lambda^{-2{,}12 \cdot 10^{-3}} \cdot V + 1{,}65 \cdot 10^{-5} \cdot \lambda^{-0{,}4} \quad . \tag{3.47}$$

The specific fuel consumption model represented in (3.47) has an error of 6,16% and R^2 of 23%. This model can be used as a first step in the design phase of an aircraft since it does not require many parameters to calculate the SFC during cruise phase.

3.4 Summary

The work presented in this chapter can be considered as a steppingstone for preliminary aircraft designs. The figures and formulas given are useful for making quick and reasonable estimations of various engine parameters.

The plot of C_a and C_b versus Bypass ratio in Figure 3.5 and Figure 3.6 proved that BPR acts directly on SFC. Also, from Figure 3.11, it is evident that the development and evolution made on BPR during the last 60 years is very remarkable. The analysis also proved that thrust reduction is highly affected by BPR. The difference between recently designed engines with high BPR and old ones is very noticeable.

Based on the data in figures from 3.3 to 3.6 the following design models are suggested

$$C_0 = (-4{,}51 \cdot 10^{-6} \cdot \ln(\lambda) + 1{,}76 \cdot 10^{-5}) \left(\frac{\text{kg}}{\text{s} \cdot \text{N}}\right) \tag{3.48}$$

$$C_{Cruise} = (-6{,}42 \cdot 10^{-6} \cdot \ln(\lambda) + 2{,}83 \cdot 10^{-5}) \left(\frac{\text{kg}}{\text{s} \cdot \text{N}}\right) \tag{3.49}$$

$$C_a = (-1{,}19 \cdot 10^{-8} \cdot \ln(\lambda) + 5{,}67 \cdot 10^{-8}) \left(\frac{\text{kg}}{\text{N} \cdot \text{m}}\right) \tag{3.50}$$

$$C_b = (-3{,}51 \cdot 10^{-6} \cdot \ln(\lambda) + 1{,}49 \cdot 10^{-5}) \left(\frac{\text{kg}}{\text{N} \cdot \text{s}}\right) \tag{3.51}$$

Besides, we can predict the specific fuel consumption at cruise phase for higher BPR from the previous figures and models. Figure 3.20 represents the prediction of SFC at cruise phase for a BPR that reaches 16. Of course, this prediction is not 100% accurate since many other parameters are not taken into consideration. However, they can present a first idea of the shape of curves for each parameter.

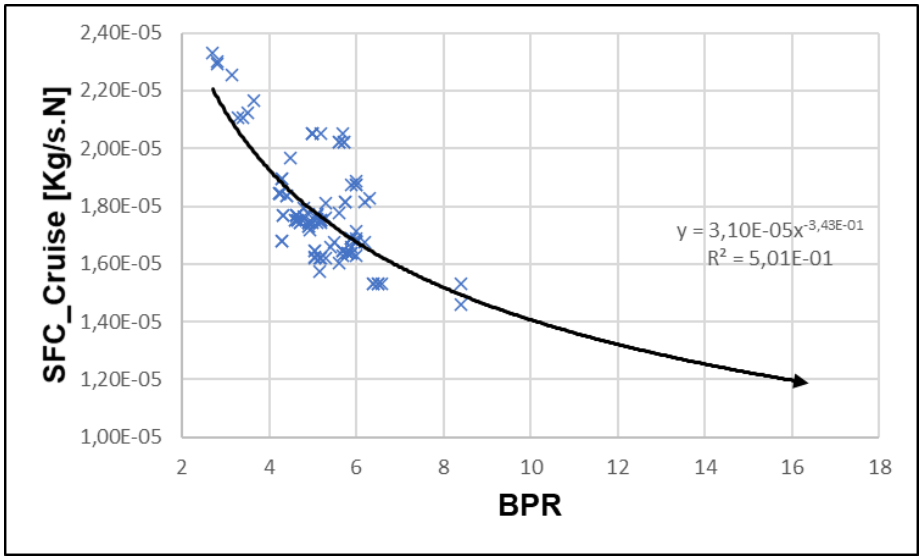

Figure 3.20 Prediction of SFC at cruise phase for higher BPR

Moreover, the preliminary sizing of an aircraft is carried out by considering requirements and constraints. The relationship between geometric and performance parameters is crucial. By Increasing the size or the mass of a turbojet engine, many other design parameters can be improved. The number of spools can be considered as a good example. Also, the increase of compressor and turbine stages can boost the thrust. However, the engine will be heavier, which can affect its compatibility with aircraft. that leads to more complications and challenging solutions needs to be found like the increase of landing gear size, the increase of the fuselage length or more etc.

From the plots, the following design models are suggested:

$$m = \left[1{,}776 \cdot 10^{-2} \cdot T_{to} \left(\frac{1}{\text{N}}\right)\right] (\text{kg}) \tag{3.52}$$

$$m = \left[8{,}01 \cdot 10^{-2} \cdot T_{cruise} \left(\frac{1}{\text{N}}\right)\right] (\text{kg}) \tag{3.53}$$

$$V = \left[4{,}311 \cdot 10^{-4} \cdot T_{TO}\left(\frac{1}{\mathrm{N}}\right)\right](\mathrm{m}^3) \tag{3.54}$$

The results obtained from linear regression and Minimum Mean Square represents a simplified linear model of the specific fuel consumption at cruise phase as a function of BPR with an error of 6.16% as shown in (3.47). This model can compete with more complex models. As an example, the model from Roux (2005) represented in the literature review has 12 input parameters and a margin of error of 6.06%.

As a matter of fact, the specific fuel consumption, Size, and mass dependencies are extremely complicated to predict with an analytical solution. Collecting a significant amount of data on modern aircraft helps to optimize flight conditions and facilitate the development of future generations of airplanes. Also, the derating of engine take-off thrust, engine age, and size need to be further investigated and understood to correlate the parameters and obtain more precise results. This work can be more optimized with an updated database.

4 Singular Value Decomposition (SVD)

4.1 SVD Fundamentals

The singular value decomposition (SVD) is initially developed by mathematicians specializing in differential geometry. Their objective was to know whether a simple bilinear form could be made equal to another by independent orthogonal transformations of the two spaces it acts on.

The core idea of the singular value decomposition is quite simple. It is based on the idea that any force vector can be decomposed into its components along the *x* and *y* axes. However, what makes the SVD special is that it extends this idea to more than one vector or point and all directions, not only along *x* and *y*.

In his research, Mandel (1982) understandably presented the singular value decomposition. He started from a linear regression model. and assumed that the model is known.

$$Y = X\beta + e \tag{4.1}$$

In (4.1), X is an $n \times p$ matrix of x_{ij} elements that represent, in our case, the engine parameters. *Y* and *e* are, on the other hand, vectors of n elements each, which *Y* consists of the measurements y_i, each of which represents the sum of two terms presented in (4.2), and e is the error term consists of e_i. And finally, β is also *a* vector of *p* elements which consists of β_i.

$$E(y_i) = \sum x_{ij}\beta_i \tag{4.2}$$

The errors e_i are assumed to be unrelated of zero mean and constant variance σ^2, the value of which is unknown.

Mandel (1982) proposed an 8×3 table of artificial data to simplify the explanation. In this case, there are three regressor variables, x_{i1}, x_{i2} and x_{i3} with x_{i1} is equal to unity for all *i*. So, the regression equation become

$$y_i = \beta_1 + \beta_2 x_{i2} + \beta_3 x_{i3} + e_i \quad . \tag{4.3}$$

The regression analysis is made to estimate the coefficients β_j and to find σ^2. Finally, the value of y_i can be predicted for any future vector of regressor variables $x = (x_1, x_2 \ldots x_p)$ and the error of every predicted value can be estimated.

Mandel (1982) also represented the regression geometrically. He proposed a regression with two variables (x_1, x_2) and plotted the design points in a plan named *D*. Then, for each design point, a segment is erected in a direction perpendicular to the plan *D* with a height of *y*. According to the author, the endpoints of the erected segment will lie to a plane *P* exactly parallel to *D*. But, because of the errors in *y*, *P* cannot be determined. However, it can be approximated by a fitted plane P_f represented in Figure 4.1.

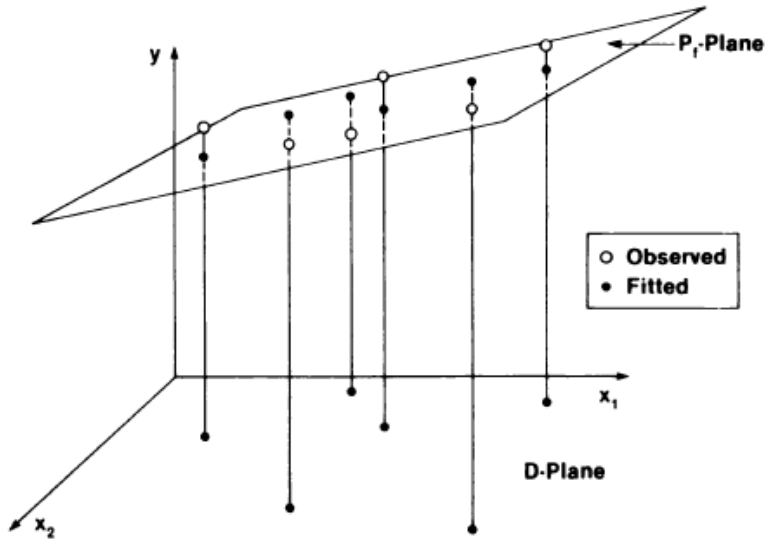

Figure 4.1 Geometric representation of a Regression surface (Mandel 1982, page 16)

4.1.1 Matrices in SVD

Mandel (1982) suggested an $n \times p$ matrix *X* with x_{ij} elements that can be expressed as shown in

$$x_{ij} = \sum_{k=1}^{r} \theta_k \, u_{ki} \, v_{ki} \quad , \tag{4.4}$$

Where $\theta_k \geq \theta_{k-1} \geq \cdots \geq \theta_r$.

In (4.4), assuming that $n \geq p$, r, which is the number of terms and referred to as a rank, must always be smaller than p. As well, *r* vectors *u* is orthogonal to each other, same for *r* vectors *v*. Also, each of these vectors has a unit length, as shown in

$$\sum_i u_{ki}^2 = \sum_i u_{ki}^2 = 1 \quad \text{for all } k. \tag{4.5}$$

So, in matrix notation, (4.4) becomes

$$X_{n\times p} = U_{n\times r}\,\theta_{r\times r}\,V_{r\times p} \quad , \tag{4.6}$$

where θ is the diagonal matrix with all θ_k are positive, the columns of the matrix U are the u vectors and the rows of V' are the v vectors. However, since U and V are orthonormal, they must obey the conditions

$$U'U = I \tag{4.7}$$

$$V'V = I \quad , \tag{4.8}$$

where I is an $r \times r$ identity matrix.
So, (4.6) can be written as

$$X_{n\times p} = U_{n\times r}\,\theta_{r\times r}\,V'_{r\times p} \quad . \tag{4.9}$$

Mandel (1982) also interpreted the SVD geometrically. Same as the linear regression interpretation, he considered an example with only two regressor variables. The author interpreted the matrix X as points in 2-dimensional space with coordinates x_{i1} and x_{i1} and joined those points to the origin so he can refer to those points as vectors.

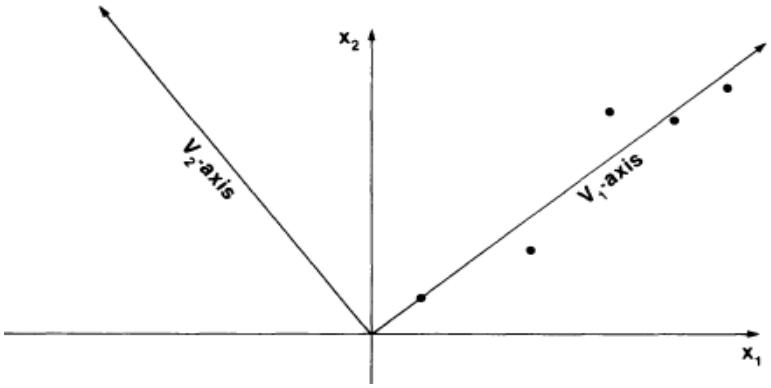

Figure 4.2 Geometric representation of Singular Value Decomposition (Mandel 1982, page 17)

The two vectors v_1 and v_1 can be considered as an alternative set of orthogonal coordinate axes. If X is transformed to the alternative coordinate system, the new coordinates of X will be given by $\theta\ u$.

The singular value decomposition approach allows reorienting the coordinate axes to obey the pattern generated by the X matrix points more closely.

4.1.2 Matrix Decomposition in SVD

As shown in (4.9), every matrix can be factorized into three other matrices, which are an orthogonal matrix *U*, a diagonal matrix θ and another orthogonal matrix V'. Physically, those three matrices can be explained as rotation (*U*), stretching (θ), and another rotation (V').
To find the singular value decomposition matrices, the eigenvalues and eigenvectors are needed to calculate the matrix *X* decomposition.

$$X = U\theta V' \tag{4.10}$$

If the elements of *X* are known, U, θ and V' can be calculated using (4.11), (4.12) and (4.13).

$$U = \{u_1, u_2\} = \left[\frac{1}{\sigma_1} X v_1, \frac{1}{\sigma_2} X v_2\right] \tag{4.11}$$

$$\theta = \begin{bmatrix} \sigma_1 & 0 \\ 0 & \sigma_2 \end{bmatrix} \tag{4.12}$$

$$V' = \{v_1, v_2\}' \tag{4.13}$$

where

σ_1, σ_2 : Singular values
v_1, v_2 : Eigenvectors

A further detailed explanation with an example of the calculation of singular value decomposition elements can be found in Appendix A.

4.2 SVD with Excel

According to Krus (2016), Singular Value Decomposition is very useful for modeling components and subsystems. It is possible to create a model with a few parameters as inputs and all the design attributes as outputs, making the design parameters estimation from given requirements fast and easy by solving the resulting system of equations.

In this subchapter, the Singular Value Decomposition method is used to calculate SFC from thrust, BPR, Altitude, OPR, Mach number, and Mass.

The calculation tool is an Excel macro created by Krus (2016). This macro is handy for the calculation of missing parameters and optimization and analysis of results. The parameters used are taken from the database created by Meier (2005). Only 131 engine models could be studied in this section due to the lack of data.

4.2.1 Error Comparison between New Equations and SVD with Excel

The first step was to gather engine models with the known parameters in an Excel spreadsheet and choose one engine to be our reference to compare the error with the analytical model. The engine chosen was CF6-50A from General Electric, as shown in the second column in Figure 4.3. Then, the analytical model was selected, which is (3.13) with an error equal to 5.25%. After that, the input matrix was created based on the known parameters, which are thrust in cruise phase, OPR at sea level, altitude, Mach number, BPR, and engine dry mass. The SFC value of the chosen engine was assumed to be unknown. Then, the initial SVD model was obtained from the Excel macro represented in Figure 4.3

	Rel error	CF6-50A	Estimate	Adjusted	Result	Average								SVD variables	w-diagonal	residual
Thrust (Cruise) [N]	69%	50042,00	15479,64	4,19	-0,17	4,36	0,295	-0,060	0,057	-0,007	0,006	-0,001	0,000	-0,32	5,42	0,48
OPR_ Sea lvl	10%	28,60	25,70	1,41	0,03	1,38	0,107	0,040	-0,034	-0,041	0,005	-0,001	0,000	0,54	2,23	0,20
Cruise Altitude [m]	0%	10668,00	10667,89	4,03	0,00	4,03	-0,009	0,023	0,008	-0,001	0,005	0,015	0,000	-0,80	0,99	0,11
Mach Number	0%	0,80	0,80	-0,10	0,00	-0,10	0,002	0,003	0,001	0,001	-0,001	0,000	0,007	-0,35	0,55	0,03
BPR+1	4%	5,40	5,20	0,72	0,04	0,68	0,125	0,173	0,013	0,013	0,004	-0,002	0,000	-0,47	0,28	0,02
Dry weight [Kg]	57%	3719,00	1596,63	3,20	-0,09	3,29	0,330	-0,028	-0,048	0,016	-0,006	0,002	0,000	-0,38	0,18	0,01
SFC (Cruise) [kg/s.N]	0%	0,00	0,00	-4,75	0,00	-4,74	-0,035	-0,037	-0,026	0,014	0,022	-0,002	0,000	-0,02	0,08	0,00
	140%															

Figure 4.3 Initial Singular Value Decomposition model

The cruise-specific fuel consumption is the parameter that will be estimated based on the SFC model in (3.13). Afterward, the Excel solver function was used to minimize the sum of relative errors. The result obtained is represented in Figure 4.4

	Rel error	CF6-50A	Estimate	Adjusted	Result	Average								SVD variables	w-diagonal	residual
Thrust (Cruise) [N]	0,01%	50042,00	50046,33	4,70	0,34	4,36	0,295	-0,060	0,057	-0,007	0,006	-0,001	0,000	0,93	5,42	0,48
OPR_ Sea lvl	0,00%	28,60	28,60	1,46	0,07	1,38	0,107	0,040	-0,034	-0,041	0,005	-0,001	0,000	-0,39	2,23	0,20
Cruise Altitude [m]	0,00%	10668,00	10668,00	4,03	0,00	4,03	-0,009	0,023	0,008	-0,001	0,005	0,015	0,000	0,68	0,99	0,11
Mach Number	0,00%	0,80	0,80	-0,10	0,00	-0,10	0,002	0,003	0,001	0,001	-0,001	0,000	0,007	-0,28	0,55	0,03
BPR+1	0,00%	5,40	5,40	0,73	0,05	0,68	0,125	0,173	0,013	0,013	0,004	-0,002	0,000	0,21	0,28	0,02
Dry weight [Kg]	0,00%	3719,00	3719,00	3,57	0,28	3,29	0,330	-0,028	-0,048	0,016	-0,006	0,002	0,000	0,78	0,18	0,01
SFC (Cruise) [kg/s.N]	7,34%	1,7985E-05	1,6664E-05	-4,78	-0,04	-4,74	-0,035	-0,037	-0,026	0,014	0,022	-0,002	0,000	-0,13	0,08	0,00
	7,35%															

Figure 4.4 Adaptation of the Singular Value Decomposition model

A value describing the SFC during the cruise phase was created based on the six known parameters. However, the error is equal to 7.34%, which is higher than the analytical solution error (5.25%).

The importance of the SVD parameters is described using the diagonal elements in the W-matrix. This diagram shows the influence of the known parameters on the result.

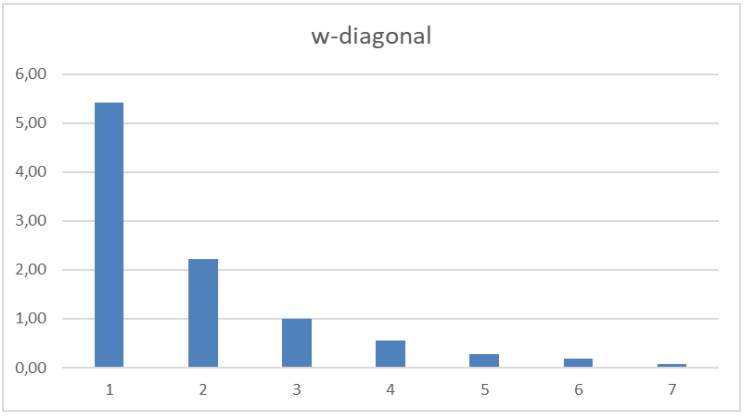

Figure 4.5 Influence of the SVD parameters (Krus 2016, page 5)

Figure 4.5 shows that the influences of the variables diminish rapidly. Here the second element influences 60% less than the first element, and the last one has almost 2% of the first element.

4.2.2 Error Comparisons in SVD with Increased Number of Input Parameters

In this subchapter, the SFC during the cruise phase is still considered unknown. The SVD is calculated using the same Excel macro from Krus (2016) but this time for different input parameters.

	Rel error	CF6-50A	Estimate	Adjusted	Result	Average							SVD variables	w-diagonal	residual
Thrust (Cruise) [N]	0%	50042,00	50041,50	4,70	0,34	4,36	0,297	-0,051	0,055	-0,006	0,001	0,000	0,95	5,28	0,48
Cruise Altitude [m]	0%	10668,00	10668,00	4,03	0,00	4,03	-0,010	0,023	0,007	-0,004	-0,016	0,000	-0,34	2,18	0,17
Mach Number	0%	0,80	0,80	-0,10	0,00	-0,10	0,002	0,003	0,000	0,000	0,000	-0,007	0,76	0,93	0,10
BPR+1	0%	5,40	5,40	0,73	0,05	0,68	0,121	0,176	0,003	-0,006	0,002	0,000	0,18	0,30	0,04
Dry weight [Kg]	0%	3719,00	3719,00	3,57	0,28	3,29	0,330	-0,022	-0,053	0,005	-0,002	0,000	-0,85	0,18	0,01
SFC (Cruise) [kg/s.N]	11%	1,838E-05	1,633E-05	-4,79	-0,04	-4,74	-0,034	-0,038	-0,026	-0,024	0,001	0,000	0,16	0,08	0,00
	11%														

Figure 4.6 Singular Value Decomposition of SFC from 5 input parameters

	Rel error	CF6-50A	Estimate	Adjusted	Result	Average							SVD variables	w-diagonal	residual
Thrust (Cruise) [N]	0,01%	50042,00	50046,33	4,70	0,34	4,36	0,295	-0,060	0,057	-0,007	0,006	-0,001	0,000	0,93	5,42	0,48
OPR_Sea lvl	0,00%	28,60	28,60	1,46	0,07	1,38	0,107	0,040	-0,034	-0,041	0,005	-0,001	0,000	-0,39	2,23	0,20
Cruise Altitude [m]	0,00%	10668,00	10668,00	4,03	0,00	4,03	-0,009	0,023	0,008	-0,001	0,005	0,015	0,000	0,68	0,99	0,11
Mach Number	0,00%	0,80	0,80	-0,10	0,00	-0,10	0,002	0,003	0,001	0,001	-0,001	0,000	0,007	-0,28	0,55	0,03
BPR+1	0,00%	5,40	5,40	0,73	0,05	0,68	0,125	0,173	0,013	0,013	0,004	-0,002	0,000	0,21	0,28	0,02
Dry weight [Kg]	0,00%	3719,00	3719,00	3,57	0,28	3,29	0,330	-0,028	-0,048	0,016	-0,006	0,002	0,000	0,78	0,18	0,01
SFC (Cruise) [kg/s.N]	7,34%	1,7985E-05	1,6664E-05	-4,78	-0,04	-4,74	-0,035	-0,037	-0,026	0,014	0,022	-0,002	0,000	-0,13	0,08	0,00
	7,35%														

Figure 4.7 Singular Value Decomposition of SFC from 6 input parameters

	Rel error	CF6-50A	Estimate	Adjusted	Result	Average											SVD variables	w-diagonal	residual
Takeoff Thrust [N]	0,00%	215000,00	214989,80	5,33	0,34	4,99	0,364	-0,018	0,029	-0,005	0,008	-0,007	0,016	-0,001	0,002	0,000	0,96	7,50	0,49
Thrust (Cruise) [N]	0,00%	50042,00	50040,57	4,70	0,34	4,36	0,293	-0,059	-0,068	-0,019	0,002	-0,006	-0,004	-0,004	0,000	0,000	-0,49	2,31	0,17
OPR_ Sea lvl	0,00%	28,60	28,60	1,46	0,07	1,39	0,106	0,038	0,030	-0,029	0,028	0,004	-0,010	-0,003	-0,003	0,000	-0,59	1,06	0,14
Mach Number	0,00%	0,80	0,80	-0,10	0,00	-0,10	0,002	0,003	-0,001	0,001	-0,001	0,000	0,001	0,000	-0,001	-0,006	0,63	0,79	0,10
BPR+1	0,00%	5,40	5,40	0,73	0,05	0,68	0,119	0,167	-0,022	0,006	-0,005	0,009	0,003	-0,007	0,002	0,000	0,75	0,50	0,08
Dry weight [Kg]	0,00%	3719,00	3719,02	3,57	0,28	3,29	0,333	-0,021	0,031	-0,010	-0,024	0,013	-0,009	0,003	0,002	0,000	0,23	0,41	0,06
Fan Diameter [m]	0,00%	2,19	2,19	0,34	0,17	0,17	0,182	0,034	0,003	0,013	-0,009	-0,008	0,001	0,002	-0,011	0,001	0,37	0,27	0,05
Length [m]	0,01%	4,65	4,65	0,67	0,20	0,47	0,127	-0,058	-0,009	0,042	0,015	0,022	0,000	-0,002	-0,001	0,000	-0,47	0,22	0,02
Width/Diameter [m]	0,00%	2,34	2,34	0,37	0,15	0,22	0,167	0,041	0,000	0,034	0,009	-0,018	-0,009	0,006	0,004	0,000	-1,65	0,14	0,02
SFC (Cruise) [kg/s.N]	4,60%	1,7985E-05	1,7158E-05	-4,77	-0,02	-4,74	-0,032	-0,035	0,028	0,017	-0,008	-0,010	-0,005	-0,016	0,000	0,000	0,54	0,07	0,01
	4,63%																		

Figure 4.8 Singular Value Decomposition of SFC from 9 input parameters

Figure 4.6 shows an error of 11% when SFC is predicted from 5 input parameters. However, Figure 4.7 and Figure 4.8 show smaller errors, respectively equal to 7.34% for six input parameters and 4.6% for nine input parameters.

Conclusively, with the increase in the number of input parameters during the calculation of the SVD, the relative error will decrease continually, and the result will be more precise. This conclusion is also proved by Lehnert (2018).

4.3 SVD with Matlab

In the following section, the SFC during the cruise phase is calculated using the SVD method. The calculation tool is MATLAB, and the input parameters are Take-off and Cruise thrust, OPR, altitude, Mach number, BPR, and engine mass. The data is taken from the same database (Meier 2005). The MATLAB code is given in Appendix B.

The model based on is a linear model represented in

$$b = A \cdot x \quad . \tag{4.14}$$

The idea is to gather the input parameters in the A matrix and the output parameter in the b vector.

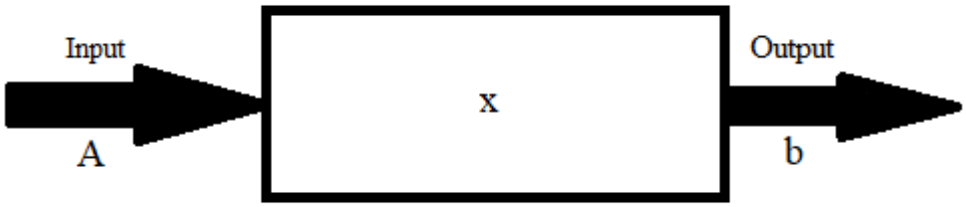

Figure 4.9 Input / Output model representation

The SVD function in MATLAB will correlate every row of the equation to solve the x vector. This method can predict the preliminary relationship between parameters and show the best fit model x for the combination of the factors to predict the output parameter.

The first step was to load the data from the Excel sheet named "SVD.xlsm". Afterward, A matrix is designated as the input parameter and b vector as the output parameter which is, in this case, SFC during the cruise phase. Next, the SVD of A was computed on MATLAB to generate the U, S and V' matrices as shown in

$$A = U \cdot S \cdot V' \quad . \tag{4.15}$$

Then, the Moore-Penrose Pseudoinverse of A was calculated as presented in

$$A^{+} = V \cdot S^{-1} \cdot U' \quad , \tag{4.16}$$

and x was solved using

$$x = A^{+} \cdot b \quad . \tag{4.17}$$

Afterward, the real SFC values and the predicted ones are plotted on the same graph, as shown in Figure 4.10.

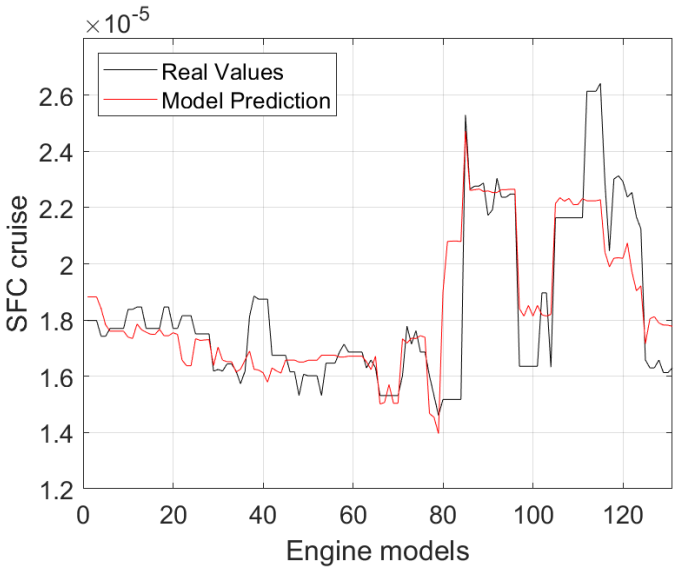

Figure 4.10 Difference between real values and predicted model

From the first observation, it is clear that the predicted model shape captures the trend variation of the real values across the data faithfully.

However, few significant outliers can be seen in Figure 4.11, representing the same data sorted by SFC values. All the engine models shown in both figures are not recent designs.

Models designed 30 years ago may not be as efficient as engines designed last ten years, which means that they do not have the same efficiency, explaining these outliers' appearance. Besides, other non-mentioned design parameters can affect the specific fuel consumption, which acts on the real values.

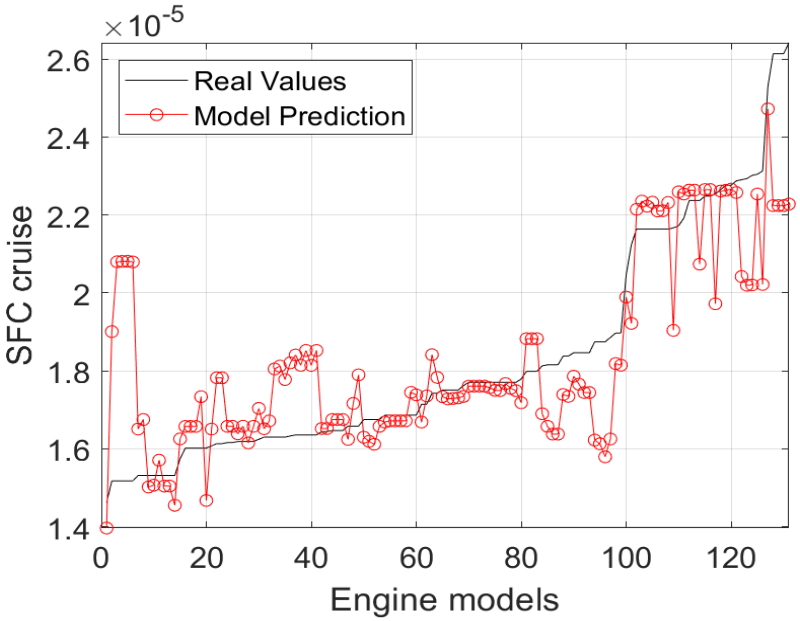

Figure 4.11 Difference between real values and predicted model sorted by SFC

The magnitude of the x vector, which is plotted on a bar graph as seen in Figure 4.12, was then used to investigate the dominant element.

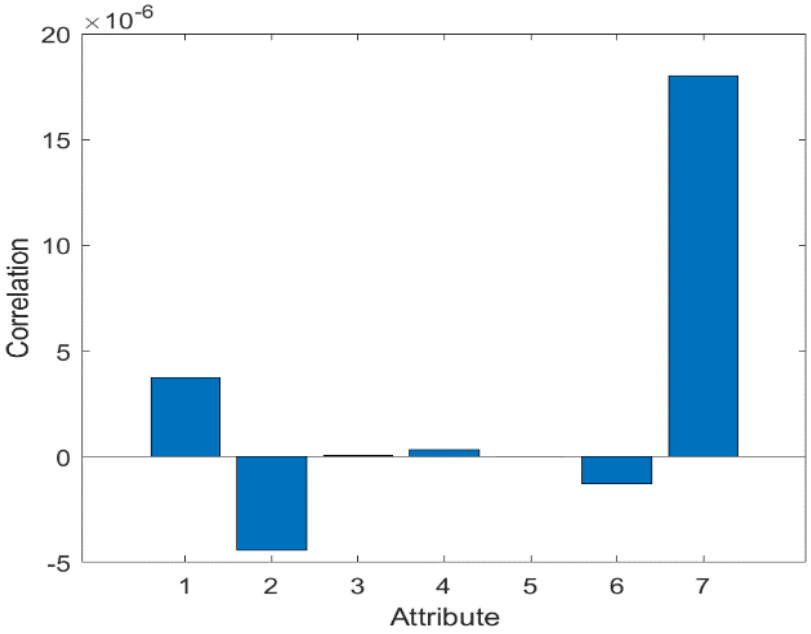

Figure 4.12 Investigation of the dominant factor acting on SFC

Figure 4.12 represents the magnitude of the slopes across each of the seven input parameters. The values of x can explain how does each attribute act on the output parameter.

Table 4.1 Input parameters represented in Figure 4.12

Attribute	Input Parameter	x-Value (slopes)
1	Take-off Thrust [N]	$3{,}734 \cdot 10^{-6}$
2	Cruise Thrust [N]	$-4{,}418 \cdot 10^{-6}$
3	OPR	$6{,}825 \cdot 10^{-8}$
4	Cruise Altitude [m]	$3{,}318 \cdot 10^{-7}$
5	Mach Number	$1{,}306 \cdot 10^{-8}$
6	BPR	$-1{,}285 \cdot 10^{-6}$
7	Engine Mass [kg]	$1{,}803 \cdot 10^{-5}$

From the bar graph, it is clear to say that some of the slopes are more important than others. Factor 7, which is the engine's mass, is positively correlated with SFC, which means that the engine will consume more fuel by increasing the mass of the aircraft. However, many other factors are anti-correlated with SFC, such as the BPR, which means that by increasing the BPR, the SFC will decrease.

Afterward, the predicted model was tested using the same data it was computed with. For that, 31 engines were hold out randomly, and the other 100 engines were used to compute the model.

Figure 4.13 represents the computation data, which are the 100 engines used to predict the model. The predicted model captures the shape of the real values, and the trends almost match perfectly. However, there is some variability caused by the outliers, as mentioned before.

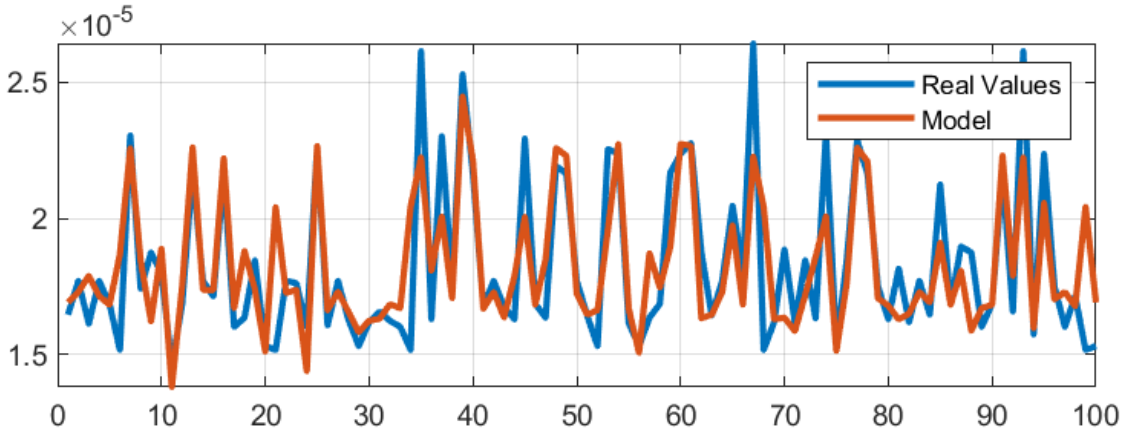

Figure 4.13 Computed Model used for 100 turbojet engines

Figure 4.14 represents the testing data which are the 31 holds out data taken randomly from the database. This data is used to test the model created in Figure 4.13.

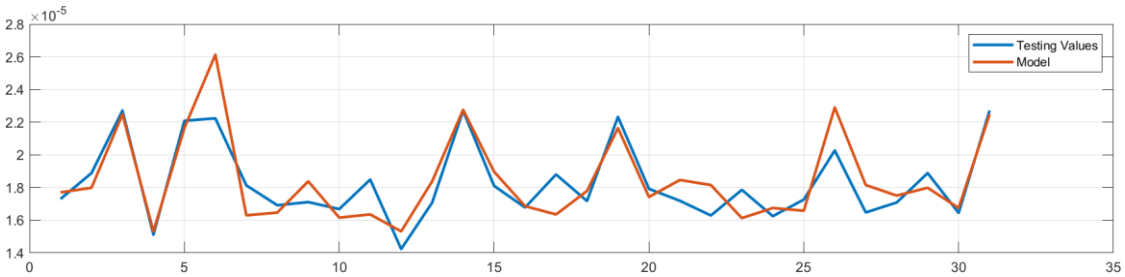

Figure 4.14 Testing the model used for 31 turbojet engines

The graph above captures the testing values more faithfully, which means that this model can be used as a preliminary design model for calculating the SFC during the cruise phase using the input parameters mentioned in Table 4.1.

4.4 Summary

The singular Value Decomposition is one of the best tools used for numerical linear algebra for data processing and analysis. It is one of the first steps in many dimensionality reductions and machine learning techniques.

In this Chapter, it has been proved that SVD can be a handy tool for establishing models for system optimization and development, estimation and completion of missing data, and modeling subsystem to estimate system characteristics based on incomplete data. This is incredibly useful during preliminary design phases where the models are not yet fully envisioned.

However, the accuracy of the SVD is low if the input parameters number is less than 9. In this case, the margin of error is equal to 7.34% which is higher than the linear regression method`s error (5.25%). On the other hand, the margin of error for a number of input parameters more than 9 is 4.6%. That justify the fact that, the increase in number of input parameters during the utilization of SVD will increase the accuracy of the results.

The SVD also allows the correlation between parameters. This means that the SVD analysis can interpret the interaction between parameters and each input parameter's influence on the output parameter.

We have seen that computation and analysis of a mathematical model are greatly facilitated using the Singular Value Decomposition. This technique also has more essential uses in dimensionality reduction and data analysis, such as evaluating experimental designs and the study of system scenarios, where quite simple models are needed to evaluate the combinations between different parameters, etc.

5 Summary and Conclusions

This thesis aims to develop simple and reliable models needed in aircraft analysis and design. Based on available parameters as input, the models must predict with a minimum error the output value as the first step in aircraft design process.

In the first part, an excel spreadsheet containing almost 718 engine models with their design parameters was created. Then, the linearity of SFC was investigated, and its factors C_a and C_b were calculated based on previously existing models. Afterward, the parameters of the engine models were correlated to investigate the variation of the factors C_a and C_b, size and engine mass vis-à-vis other engine parameters. In the end, new models were deduced based on linear regression and minimum mean square error in Excel. The obtained result is a linear model of SFC at cruise phase as function of BPR. This model has an error of 6.16% and an R^2 of 0,23. This simplified model can compete with more complex models such as Torenbeek (1997) from (2.3) which require more input parameters to measure the SFC and have an error of 6.6% at cruise phase and the model from Roux (2005) from (2.4) which require 12 input parameters with an error of 6.06%.

Next, the numerical method of SVD was applied to calculate the SFC. Firstly, an Excel macro created by Krus (2016) is used to define the calculation model. Then, for the same input parameters, it has been verified that this method provides a significantly less accurate result of the SFC estimation ($e = 7.37\%$) than the analytical method of the linear regression ($e = 5.25\%$). On the other hand, it has been proven that a higher-value result from the SVD is obtained when 9 or more input parameters can be included ($e = 4{,}6\%$). Secondly, a MATLAB code was applied to compute another calculation model of the SFC. From the results, it has been shown that the engine mass and size are the most influencing parameters on SFC.

The singular value decomposition could be an accurate and valuable tool during the preliminary design phase. This function allows the designer to model subsystems to estimate system characteristics based on incomplete data. However, the use of SVD requires many further investigations since the results are just predictions. Also, many parameters will be unknown during the development of new propulsion systems, increasing the error margin.

The models developed are relatively simple. However, engine parameter behavior investigations are too complicated without simplified models, and an analytical solution is almost impossible. That is why this kind of research is crucial during the first steps of the design phase of future generations of aircraft.

The possibilities for improving and continuing this work are relatively open and numerous. First, an inquiry is needed to classify and assess whether the SVD method is sufficiently

precise for specific applications. Moreover, the data used in this thesis are not recent, and since the aeronautical field is always evolving, a simulation with the newest data is needed to obtain better results and analysis.

List of References

ANDERSON, John D., 1989. *Introduction to Flight*. New York, USA: McGraw-Hill.
Available from: https://cutt.ly/zWMc98X

BARTEL, Matthias, YOUNG M, Trevor, 2008. Simplified Thrust and Fuel Consumption Models for Modern Two-Shaft Turbofan Engines. In: *Journal of Aircraft*, vol. 45 no. 4, pp. 1450-1456.
Available from: https://doi.org/10.2514/1.35589 (Closed Access)

BENSEL, Arthur, 2018. *Characteristics of the Specific Fuel Consumption for Jet Engines*. Hamburg University of Applied Sciences.
Availalble from: https://nbn-resolving.org/urn:nbn:de:gbv:18302-aero2018-08-31.016

BOSE, Tarit, 2012. *Airbreathing Propulsion: An Introduction*. Appendix: Engine Data Tables. pp. 268-309.
Available from: https://doi.org/10.1007/978-1-4614-3532-7

DANKANICH, Andrew, PETERS, David, 2017. *Turbofan Engine Bypass Ratio as a Function of Thrust and Fuel Flow*. Washington University in St.Louis, USA.
Available from: https://cutt.ly/kjxj0aN
Archived at: https://perma.cc/TN8L-6WJC

Direction Generale de l'Aviation Civile (DGAC), 2020. Noise Certification Database. Paris, France.
Available from: http://noisedb.stac.aviation-civile.gouv.fr/bdd

DIK, A., BITEN, N., ZACCARIA, V., ASLANIDOU, I., KYPRIANIDIS, K., 2017. Conceptual Design of a 3-Shaft Turbofan Engine with Reduced Fuel Consumption for 2025. In: *The 15th International Symposium on District Heating and Cooling*, Sweden, vol. 142.
Available from: https://doi.org/10.1016/j.egypro.2017.12.556

FABIAN, John, CELESTINA, Mark, KULKARNI, Sameer, 2012. *NASA Environmentally Responsible Aviation High Overall Pressure Ratio Compressor Research – Pre-Test CFD*. Ohio, USA.
Available from: https://doi.org/10.2514/6.2012-4040
Open Access at: https://core.ac.uk/download/pdf/10572377.pdf
Archived at: https://perma.cc/manage/create?folder=52363-110726

FREIRE, Valdi, RIBEIRO, Raphael, LACAVA, Pedro, 2019. Turbofan Engine Performance Optimization Based on Aircraft Cruise Thrust Level. In: *Journal of the Brazilian Society of Mechanical Sciences and Engineering*, vol. 41, no. 1, art. 64, Brazil: Elsevier.
Available from: https://doi.org/10.1007/s40430-018-1562-1 (Closed Access)

GAO, Jian-hua, HUANG, Ying-yun, 2011. Modeling and Simulation of an Aero Turbojet Engine with GasTurb. In: *International Conference on Intelligence Science and Information Engineering*, Wuhan, China, pp. 295-298.
Available from: https://doi.org/10.1109/ISIE.2011.149

GUHA, Abhijit, 2001. *Optimum Fan Pressure Ratio for Bypass Engines with Separate or Mixed Exhaust Streams.* University of Bristol, Bristol, England, vol. 17, no. 5.
Availalble from: https://arc.aiaa.org/doi/10.2514/2.5852

HERRMANN, Steffen, 2010. *Untersuchung des Einflusses der Motorenzahl auf die Wirtschaftlichkeit eines Verkehrsflugzeuges unter Berücksichtigung eines optimalen Bypassverhältnisses.* Diplomarbeit. Institut für luft- und Raumfahrt, TU Berlin.
Availalble from: https://cutt.ly/3WMhkFD

JENKINSON, Lloyd, SIMPKIN, Paul, RHODES, Darren, 1999. *Civil Jet Aircraft Design.* London, United Kingdom: Arnold.
Archived at: https://perma.cc/2VMC-J2KQ

JENKINSON, Lloyd, 2001. *Database for Civil Jet Aircraft Design.*
Available from : https://cutt.ly/ljxlzv0

KRUS, Petter, 2016. *Models Based on Singular Value Decomposition for Aircraft Design*. Department of Management and Engineering, Division of Fluid and Mechatronic Systems, Linköping University, Sweden.
Available from: https://bit.ly/2O4hFt5

LEHNERT, Jan, 2018. *Methoden zur Ermittlung des Betriebsleermassenanteils im Flugzeugentwurf.* HAW-Hamburg. Germany.
Available from: https://cutt.ly/ilDnp9i
Archived at: http://library.ProfScholz.de

MANDEL, John, 1982. *Use of the Singular Value Decomposition in Regression Analysis*. American Statistician, vol. 36, no. 1, pp. 15-24.
Available from: https://bit.ly/3pqDbW0

MATTINGLY, Jack D, 1996. *Elements of Gas Turbine Propulsion.* Library of Congress, New York, USA.
Available from: https://www.amazon.de/dp/0071145214
Archived at: https://perma.cc/9XES-3BJC

MATTINGLY, Jack D, HEISER, William H, PRATT, David T, 2002. *Aircraft Engine Design, Second Edition.* The American Institute of Aeronautics and Astronautics, Reston Virginia, USA.
Archived at: https://doi.org/10.2514/4.861444 (Closed Access)

MCLEOD, Saul, 2019. What a P-Value Tells you About Statistical Significance. In: *Simply Psychology*.
Available from: https://www.simplypsychology.org/p-value.html
Archived at: https://perma.cc/D3Q7-38TJ

MEIER, Nathan, 2005. Jet Engine Specification Database.
Archived at: https://cutt.ly/SWMfMWu

NAJJAR, Yousef, BALAWNEH, Ibrahim, 2015. Optimization of Gas Turbines for Sustainable Turbojet Propulsion. In: *Propulsion and Power Research*, Irbid, Jordan, vol. 4, no. 2, pp. 114-121.
Archived at: https://doi.org/10.1016/j.jppr.2015.05.004

OJHA, S. K., 1995. *Flight Performance of Aircraft*. Indian Institute of Technology, Bombay, India. American Institute of Aeronautics and Astronautics,
Available from: https://cutt.ly/flDmSGk (Closed Access)

PATEL, Vivek, SAVASNI, Vimal, MUDGAL, Anurag, 2018. *Efficiency, Thrust, and Fuel Consumption Optimization of a Subsonic/Sonic Turbojet Engine.* Pandit Deendayal Petroleum University, Gujarat, India, vol. 144, no. 1, pp. 992-1002.
Available from: https://doi.org/10.1016/j.energy.2017.12.080

ROUX, Elodie, 2005. *Pour une Approche Analytique de la Dynamique du Vol*. In : Onera Cert. Toulouse, France.
Available from: https://cutt.ly/8jxzEBc

ROUX, Elodie, 2007a. *Turbofan and Turbojet Engines Database Handbook.* In: Editions Elodie Roux.
Available from: https://cutt.ly/bjxzKCP
Archived at: https://cutt.ly/xjxzZlI

ROUX, E, 2007b. *Avions Civils a Reaction: Plan 3 Vues et Données Caractéristiques*. In : Editions Elodie Roux.
Available from: https://cutt.ly/SjxkDL3

SCHOLZ, Dieter, 2015. Aircraft Design. Lecture Notes. Hamburg University of Applied Sciences.
Available from: http://hoou.ProfScholz.de

SCHOLZ, Dieter, 2017. *Der spezifische Kraftstoffverbrauch von Flugtriebwerken (TSFC und PSFC)*. Memo. Aircraft Design and Systems Group (Aero), Hamburg University of Applied Sciences. 2017-07-15.
Available from: https://doi.org/10.31224/osf.io/gyt7u
Available from: http://reports-at-aero.ProfScholz.de

SCHOLZ, Dieter, 2019a. *Tafelbilder zur Volesung Flugmechanik*. Hamburg University of Applied Sciences.
Availalble from: https://cutt.ly/HWMlsh2

SCHOLZ, Dieter, 2019b. *Tabellenkalkulation zur Berechnung von SFC (TSFC und PSFC) für Jets (Herrmann)*. Excel Spreadsheet. Hamburg University of Applied Sciences.
Availalble from : https://cutt.ly/vWMl302

SCHULZ, Oliver, 2007. *Assessment of Numerical Models for Thrust and Specific Fuel Consumption for Turbofan Engines.* Hamburg University of Applied Sciences.
Available form: https://cutt.ly/mW2owe5
Available from: http://library.ProfScholz.de
Archived at: https://perma.cc/9ZZQ-74RM

SCHUTTE, Jeffrey, 2009. *Simultaneous Multi-Design Point Approach to the Gas Turbine on Design Cycle Analysis for Aircraft Engines.* Georgia Institute of Technology, Atlanta, USA.
Available from: http://hdl.handle.net/1853/28169

SVOBODA, Charlie, 2000. *Aircraft Design. Turbofan Engine Database as a Preliminary Design Tool*. University of Kansas, USA, vol. 3, no. 1, pp. 17-31.
Archived at: https://cutt.ly/8jxxpMQ

TORENBEEK, Egbert, 1997. *Cruise Performance and Range Prediction Reconsidered. In: Progress in Aerospace Sciences*. Delft University of Technology. Delft, The Netherlands. vol. 33, no. 5-6, pp. 285-321.
Archived at: https://cutt.ly/ajxxgW6

YOUNG, J. B., WILCOCKT, R., HORLOCK, J., 2005. The Effect of Turbine Blade Cooling on the Cycle Efficiency of Gas Turbine Power Cycles. In: *Journal of Engineering for Gas Turbines and Power*. vol. 127, no. 1, pp. 109-120.
Available from: https://doi.org/10.1115/1.1805549 (Closed Access)

Appendix A – Example of Calculation of Singular Value Decomposition Elements

If we have a matrix X with 3×2 elements with random numbers.

$$X = \begin{bmatrix} 1 & 1 \\ 0 & 1 \\ -1 & 1 \end{bmatrix}$$

The first step is to calculate the eigenvalues and the eigenvectors of the matrix X. For that, we must multiply the matrix by its transpose.

$$X^T X = \begin{bmatrix} 1 & 0 & -1 \\ 1 & 1 & 1 \end{bmatrix} \begin{bmatrix} 1 & 1 \\ 0 & 1 \\ -1 & 1 \end{bmatrix} = \begin{bmatrix} 2 & 0 \\ 0 & 3 \end{bmatrix}$$

Then, we calculate the eigenvalues of $X^T X$

$$|X^T X - \lambda I| = \begin{bmatrix} 2-\lambda & 0 \\ 0 & 3-\lambda \end{bmatrix} = 0$$

and we calculate its determinant to find $\lambda_1 = 3$ and $\lambda_2 = 2$. After that, we calculate the singular values of $X^T X$ which are the square roots of the non-zero eigenvalues of X

$$\sigma_1 = \sqrt{\lambda_1} = \sqrt{3}\,;\ \sigma_2 = \sqrt{\lambda_2} = \sqrt{2}$$

Now we need to find the eigenvectors of $X^T X$ using the eigenvalues λ_1 and λ_2

$$v_1 = \begin{bmatrix} 0 \\ 1 \end{bmatrix}\ ; v_2 = \begin{bmatrix} 1 \\ 0 \end{bmatrix}$$

After that, we can use the eigenvalue, singular values, and eigenvectors to calculate U, θ and V'.

$$U = \{u_1, u_2, u_3\} = \left[\frac{1}{\sigma_1} X v_1, \frac{1}{\sigma_2} X v_2, u_3\right]$$

where

$$u_1 = \frac{1}{\sigma_1} X v_1 = \frac{1}{\sqrt{3}} \begin{bmatrix} 1 & 1 \\ 0 & 1 \\ -1 & 1 \end{bmatrix} \begin{bmatrix} 0 \\ 1 \end{bmatrix} = \begin{bmatrix} 1/\sqrt{3} \\ 1/\sqrt{3} \\ 1/\sqrt{3} \end{bmatrix}$$

$$u_2 = \frac{1}{\sigma_2} X v_2 = \frac{1}{\sqrt{2}} \begin{bmatrix} 1 & 1 \\ 0 & 1 \\ -1 & 1 \end{bmatrix} \begin{bmatrix} 1 \\ 0 \end{bmatrix} = \begin{bmatrix} 1/\sqrt{2} \\ 0 \\ -1/\sqrt{2} \end{bmatrix}$$

u_3 can be found using the Gram-Schmidt orthogonalization process.

$$u_3 = \begin{bmatrix} 1/\sqrt{6} \\ -2/\sqrt{6} \\ 1/\sqrt{6} \end{bmatrix}$$

$$\theta = I \cdot \begin{bmatrix} \sigma_1 & 0 \\ 0 & \sigma_2 \end{bmatrix}$$

and

$$V = \{v_1, v_2\} = \begin{bmatrix} 0 & 1 \\ 1 & 0 \end{bmatrix}$$

So

$$V' = \begin{bmatrix} 0 & 1 \\ 1 & 0 \end{bmatrix}$$

Finally, we obtained the singular value decomposition of matrix *X*.

$$X = \begin{bmatrix} 1/\sqrt{3} & 1/\sqrt{2} & 1/\sqrt{6} \\ 1/\sqrt{3} & 0 & -2/\sqrt{6} \\ 1/\sqrt{3} & -1/\sqrt{2} & 1/\sqrt{6} \end{bmatrix} \begin{bmatrix} \sqrt{3} & 0 \\ 0 & \sqrt{2} \\ 0 & 0 \end{bmatrix} \begin{bmatrix} 0 & 1 \\ 1 & 0 \end{bmatrix}$$

X = U θ V'

Appendix B – SVD MATLAB Code

To ensure the compilation of the code, each part of it needs to be executed separately according to the expected result.

```
clear all, close all, clc

%% Import data from spreadsheet

%    Workbook: C:\Users\mouss\OneDrive\Bureau\Master Thesis Calculation
Papers\SVD.xlsm

%% Setup the Import Options and import the data
opts = spreadsheetImportOptions("NumVariables", 16);

% Specify sheet and range
opts.Sheet = "Database";
opts.DataRange = "A5:P135";

% Specify column names and types
opts.VariableNames = ["Manufacturer", "Model", "BPR", "CruiseAltitudeft",
"SFCh0M0kgsN", "TakeoffThrustN", "ThrustCruiseN", "OPR_Sealvl",
"CruiseAltitudem", "MachNumber", "BPR1", "DryweightKg", "FanDiameterm",
"Lengthm", "WidthDiameterm", "SFCCruisekgsN"];
opts.VariableTypes = ["categorical", "string", "double", "double",
"double", "double", "double", "double", "double", "double", "double",
"double", "double", "double", "double", "double"];

%% Format Changing
format shortG

%% Import the data
data = xlsread("C:\Users\mouss\OneDrive\Bureau\Master Thesis Calculation
Papers\Singular Value Decomposition\SVD.xlsm"
);
A = data(:,4:10);
b = data(:,14);

% Solving Ax=b using the SVD
[U,S,V] = svd(A,'econ');
x = V*inv(S)*U'*b;


%% Plot data

plot(b,'k');      %Figure 1
hold on, grid on
plot(A*x,'r');
set(gca,'FontSize',14)
xlim([0 size(A,1)])
l1 = legend('Real Values','Model Prediction')
set(l1,'Location','Northwest')
xlabel('Engine models')
ylabel('SFC cruise')

figure
[b sortind] = sort(b);     %Figure 2
plot(b,'k')
```

```
hold on ,grid on
plot(A(sortind,:)*x,'r-o')
l2 = legend('Real Values','Model Prediction')
set(l2,'Location','Northwest')
set(gca,'FontSize',15)
xlim([0 size(A,1)])
set(l1,'FontSize',18)
grid on
xlabel('Engine models')
ylabel('SFC cruise')

%% Importance of each parameter

for i=1:size(A,2)
    Astd=std(A(:,i));
    A(:,i)=A(:,i)/Astd;
end
A(:,end) = ones(size(A,1),1);
format shortG
x = regress(b,A)
figure
bar(x(1:7))
xlabel('Attribute'),ylabel('Correlation')
set(gca,'FontSize',13)
set(gcf,'Position',[100 100 600 500])

%% Data Testing

n=100;   %Number of data used to build the model

data = xlsread("C:\Users\mouss\OneDrive\Bureau\Master Thesis Calculation
Papers\Singular Value Decomposition\SVD.xlsm"
);
A = data(:,4:10);
b = data(:,14);

p = randperm(131);
b = b(p);
A = A(p,:);
btaining = b(1:n);
Atraining = A(1:n,:);
x = regress(btaining,Atraining);

btest = A(n+1:end,:)*x;
norm(btest-b(n+1:end))

subplot(2,1,1)
plot(btaining,'linewidth',2)
hold on, grid on
plot(Atraining*x,'Linewidth',2)
legend('Real Values','Model')

% figure
subplot(2,1,2)
plot(btest,'LineWidth',2)
hold on, grid on
plot(b(n+1:end),'LineWidth',2)
legend('Testing Values','Model')
```